

Supplementary Information

Structural and optical investigations of charge transfer complexes involving the radical anions of TCNQ and F₄TCNQ

Ashley L. Sutton,^a Brendan F. Abrahams,^{*a} Deanna M. D'Alessandro,^b Timothy A. Hudson,^a Richard Robson,^{*a} and Pavel M. Usov^b

A School of Chemistry, University of Melbourne, Victoria 3010, Australia

B School of Chemistry, University of Sydney, NSW 2006, Australia,

Email: bfa@unimelb.edu.au; r.robson@unimelb.edu.au; Fax: +61 3 9347 5180.

S1 – Full Synthetic Details

S2 – Longitudinal and transverse offsets, dimer separations and acceptor redox potentials

S3 – X-Ray Diffraction Powder Patterns

S4 – EPR Spectra

S5 – Supplementary figures

S6 - Supplementary Vis-NIR solid-state diffuse reflectance spectra and corresponding Tauc plots

S1 – Full Synthetic Details

[(1)TCNQ]: A solution of **(1)I** (12.7 mg, 0.047 mmol) in methanol (1 mL) was layered onto a solution of LiTCNQ (10.0mg, 0.047 mmol) in DMF (0.5 mL). Purple crystals of **[(1)TCNQ]** separated from the solution overnight (8.4 mg, 26 %). Crystals suitable for X-ray diffraction were obtained through slow oxidation of the TCNQH₂ precursor. A suspension of TCNQH₂ (25.0 mg, 0.12 mmol) and Li(OAc) (32.7 mg, 0.32 mmol) in methanol (2 mL) was added to a solution of **(1)I** (32.5 mg, 0.12 mmol) in methanol (2 mL). IR (KBr): 3441, 2184, 2172, 2147, 1578, 1504, 1356, 1180, 983, 827, 475 cm⁻¹.

[(2)TCNQ]: A solution of **(2)I** (12.7 mg, 0.047 mmol) in methanol (1 mL) was layered onto a solution of LiTCNQ (10.0mg, 0.047 mmol) in DMF (0.5 mL). Purple crystals of **[(2)TCNQ]** separated from the solution overnight (5.2 mg, 32 %). Crystals suitable for x-ray diffraction were obtained through slow oxidation of the TCNQH₂ precursor. A solution of TCNQH₂ (25.0 mg, 0.12 mmol) and Li(OAc) (32.7 mg, 0.32 mmol) in methanol (2 mL) was added to a solution of **(2)I** (32.5 mg, 0.12 mmol) in methanol (2 mL). Elemental analysis Calcd C₂₂H₁₄N₅: C, 75.85; H, 4.05; N, 20.10; Found: C, 75.78; H, 4.08; N, 20.22 %. IR (KBr): 3445, 2924, 2182, 2169, 1579, 1504, 1356, 1181, 770 cm⁻¹.

[(2)F₄TCNQ]: A solution of LiF₄TCNQ (10.0 mg, 0.035 mmol) in methanol (1 mL) was added to a solution of **(2)I** (9.5 mg, 0.035 mmol) in methanol (1 mL). Dark purple crystals of **[(2)F₄TCNQ]** separated from the solution overnight (8.0 mg, 54 %). Crystals suitable for x-ray diffraction were obtained through slow oxidation of the F₄TCNQH₂ precursor. A solution of F₄TCNQH₂ (8.3 mg, 0.03 mmol) and Li(OAc) (8.2 mg, 0.08 mmol) in methanol (2 mL) was added to a solution of **(2)I** (8.1 mg, 0.03 mmol) in methanol (2 mL). IR (KBr): 3443, 2920, 2851, 2196, 2177, 1635, 2177, 1635, 1538, 1501, 1390, 1340, 1169, 970, 821, 775 cm⁻¹.

[(3)TCNQ]: A solution of **(3)I** (12.6 mg, 0.047 mmol) in methanol (1 mL) was layered onto a solution of LiTCNQ (10.0mg, 0.047 mmol) in DMF (0.5 mL). Purple crystals of **[(3)TCNQ]** separated from the solution overnight (12.8 mg, 58 %). Crystals suitable for X-ray diffraction were obtained through slow oxidation of the TCNQH₂ precursor. A suspension of TCNQH₂ (25.0 mg, 0.12 mmol) and Li(OAc) (32.7 mg, 0.32 mmol) in methanol (2 mL) was added to a solution of **(3)I** (41.2 mg, 0.12 mmol) in methanol (2 mL). IR (KBr): 3397, 2182, 2153, 1580, 1528, 1500, 1351, 1178, 1084, 857, 713 cm⁻¹.

[(4)TCNQ₂]: A solution of (4)Cl₂ (5.2 mg, 0.012 mmol) in methanol (1 mL) was layered onto a solution LiTCNQ (5.0 mg, 0.024 mmol) in DMF (0.5 mL). Dark purple crystals suitable for single crystal x-ray diffraction of [(4)TCNQ₂] separated from the solution overnight (5.5 mg, 59 %). IR (KBr): 3442, 2922, 2177, 2155, 1639, 1579, 1500, 1343, 1175, 824, 758, 477 cm⁻¹.

[(5)F₄TCNQ]: A solution of LiF₄TCNQ (10.0 mg, 0.035 mmol) in methanol (1 mL) was added to a solution of (5)Br (11.1 mg, 0.035 mmol) in methanol (2 mL). Purple/blue crystal of [(5)TCNQ] separated from the solution overnight (12.3 mg, 68 %). Crystals suitable for X-ray diffraction were obtained through slow oxidation of the F₄TCNQH₂ precursor. A suspension of F₄TCNQH₂ (8.3 mg, 0.03 mmol) in methanol (2 mL) was added to a solution of (5)Br (9.5 mg, 0.03 mmol) in methanol (1 mL). IR (KBr): 3443, 2924, 2193, 2176, 1634, 1533, 1396, 1387, 969, 708 cm⁻¹.

[(6)TCNQ]: A solution of LiTCNQ (5.0 mg, 0.024 mmol) in methanol (1 mL) was added to a solution of (6)Br (7.6mg, 0.024 mmol) in methanol (1 mL). Dark purple crystals suitable for single crystal x-ray diffraction of [(6)TCNQ] separated from the solution overnight (5.6 mg, 53 %). IR (KBr): 3443, 2188, 2174, 2148, 1587, 1530, 1508, 1481, 1360, 1183, 823, 479 cm⁻¹.

[(7)TCNQ]: A solution of LiTCNQ (10.0 mg, 0.047 mmol) in methanol (1 mL) was added to a solution of (7)Br (14.5 mg, 0.047 mmol) in methanol (2 mL). Purple crystals with a metallic-like sheen of [(7)TCNQ] separated from the solution overnight (10.4 mg, 51 %). Crystals suitable for X-ray diffraction were obtained through slow oxidation of the TCNQH₂ precursor. A suspension of TCNQH₂ (25.0 mg, 0.12 mmol) and Li(OAc) (32.7 mg, 0.32 mmol) in methanol (4 mL) was added to a solution of (7)Br (37.1 mg, 0.12 mmol) in methanol (4 mL). Elemental analysis Calcd C₂₅H₁₇N₆O₂: C, 69.28; H, 3.95; N, 19.39; Found: C, 69.23; H, 4.00; N, 19.56 %. IR (KBr): 3442, 2922, 2360, 2343, 2173, 2131, 1701, 1514, 1348, 1189, 1162, 668 cm⁻¹.

[(8)TCNQ]: A solution of LiTCNQ (10.0 mg, 0.047 mmol) in methanol (1 mL) was added to a solution of (8)Br (13.9 mg, 0.047 mmol) in methanol (2 mL). Dark purple crystals of [(8)TCNQ] separated from the solution overnight (4.4 mg, 10 %). Crystals suitable for x-ray

diffraction were obtained through slow oxidation of the TCNQH₂ precursor. IR (KBr): 3442, 2993, 2185, 2170, 2138, 1630, 1579, 1535, 1504, 1347, 1184, 829, 696 cm⁻¹.

[(9)TCNQ₂]: A solution of LiTCNQ (10.0 mg, 0.047 mmol) in methanol (1 mL) was added to a solution of **(9)Cl** (8.0 mg, 0.024 mmol) in methanol (2 mL). Black/dark blue crystals of **[(9)TCNQ₂]** separated from the solution overnight (7.4 mg, 23 %). Crystals suitable for single crystal x-ray diffraction were obtained through slow oxidation of the TCNQH₂ precursor. A suspension of TCNQH₂ (25.0 mg, 0.12 mmol) and Li(OAc) (32.7 mg, 0.32 mmol) in methanol (4 mL) was added to a solution of **(9)Cl** (40.7 mg, 0.12 mmol) in methanol (4 mL). Elemental analysis Calcd C₄₀H₂₈N₁₂: C, 70.99; H, 4.17; N, 24.84; Found: C, 70.83; H, 4.00; N, 25.01 %. IR (KBr): 3433, 3122, 3083, 2187, 2174, 2159, 1581, 1506, 1347, 1173, 821, 480 cm⁻¹.

[(10)TCNQ]: A solution of LiTCNQ (10.0 mg, 0.047 mmol) in methanol (1 mL) was added to a solution of **(10)BF₄** (14.2 mg, 0.047 mmol) in methanol (2 mL). Dark purple crystals of **[(10)TCNQ]** separated from the solution overnight. Crystals suitable for single crystal x-ray diffraction were obtained through slow oxidation of the TCNQH₂ precursor. A suspension of TCNQH₂ (25.0 mg, 0.12 mmol) in methanol (4 mL) was added a solution of proton sponge (25.7 mg, 0.12 mmol) in methanol (4 mL). Elemental analysis Calcd C₂₆H₂₃N₆: C, 74.44; H, 5.53; N, 20.03; Found: C, 74.68; H, 5.74; N, 20.14 %. IR (KBr): cm⁻¹. IR (KBr): 3450, 2923, 2852, 2178, 2152, 1637, 1505, 1360, 770 cm⁻¹.

[(10)F₄TCNQ]: A solution of LiF₄TCNQ (10.0 mg, 0.035 mmol) in methanol (1 mL) was added to a solution of **(10)BF₄** (10.6 mg, 0.035 mmol) in methanol (2 mL). Dark blue crystal of **[(10)F₄TCNQ]** separated from the solution overnight (13.7 mg, 80 %). Crystals suitable for single crystal x-ray diffraction were obtained through slow oxidation of the F₄TCNQH₂ precursor. A suspension of F₄TCNQH₂ (8.3 mg, 0.03 mmol) in methanol (2 mL) was added to a solution of proton sponge (6.4 mg, 0.03 mmol) in methanol (1 mL). Elemental analysis Calcd C₂₆H₁₉F₄N₆: C, 63.54; H, 3.90; N, 17.10; Found: C, 63.56; H, 3.91; N, 17.11 %. IR (KBr): 3442, 2923, 2853, 2191, 2169, 1626, 1499, 1336, 1142, 967, 773 cm⁻¹.

S2 – Longitudinal and transverse offsets, dimer separations and acceptor redox potentials

Table S2.1 – Longitudinal and transverse offsets, intradimer separations and acceptor redox potentials for each reported TCNQ based charge-transfer complex.

Packing Type	Compound	D* (Å)	L* (Å)	T* (Å)	Cation Reduction Potential (mV) vs (Fc/Fc ⁺)
I	[(1)TCNQ]	3.03	2.10	0.14	- 1295 ^a
	[(2)TCNQ]	3.00	2.12	0.11	- 1303 ^a
	[(2)F ₄ TCNQ]	3.11	0.13	0.74	- 1303 ^a
	[(3)TCNQ]	3.13	0.17	0.91	- 1293
	[(4)TCNQ ₂]	3.12	0.06	0.86	- 1497 ^a
II	[(5)F ₄ TCNQ]	3.07	0.07	0.92	- 1395
	[(6)TCNQ]	3.16	2.10	0.29	- 1385 ^a
	[(7)TCNQ]	3.19	0.02	0.88	- 1404 ^a
	[(8)TCNQ]	3.04	2.02	0.16	- 1232 ^a
	[(9)TCNQ ₂]	3.12	0.03	0.98	- 1245 ^a
		3.11	2.14	0.35	
III	[(10)TCNQ]	3.53	5.72	0.89	- 1250 ^a
	[(10)F ₄ TCNQ]	3.59	6.20	0.04	- 1250 ^a

* Longitudinal, transverse offsets and dimer separations were calculated as described in J. Huang, S. Kingsbury and M. Kertesz, *Physical chemistry chemical physics : PCCP*, 2008, **10**, 2625-2635. ^a The given redox potential is the Epc as the process is irreversible.

S3 – X-Ray Diffraction Powder Patterns

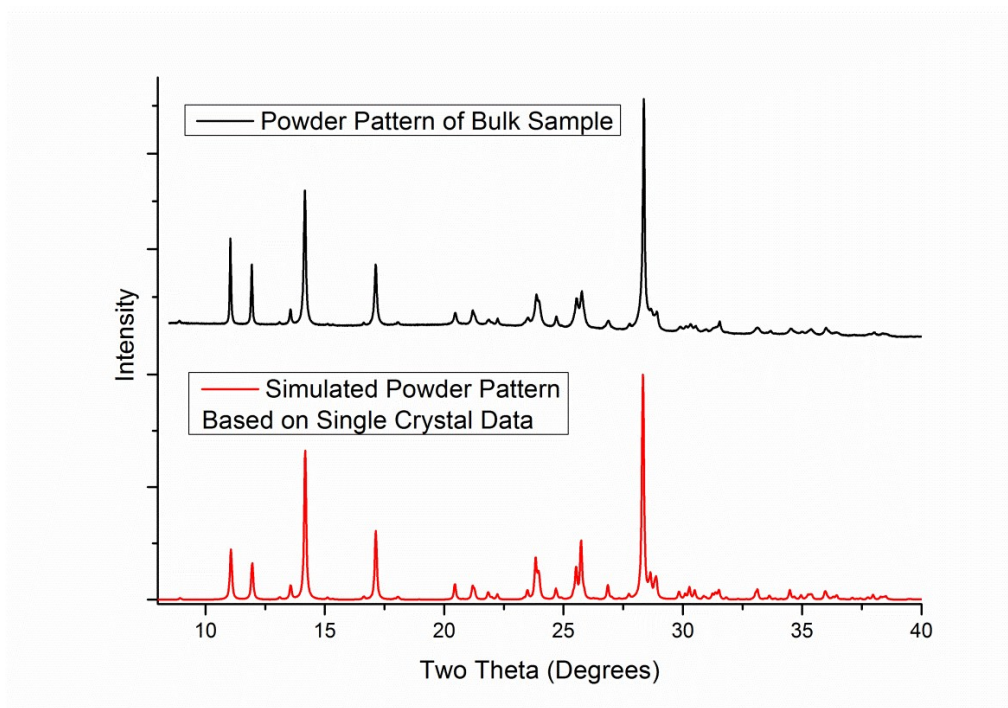


Figure S3.1. Bulk powder pattern and the simulated powder pattern for [(1)TCNQ]. Data collected on the Powder Diffraction Beamline at the Australian Synchrotron at 130 K.

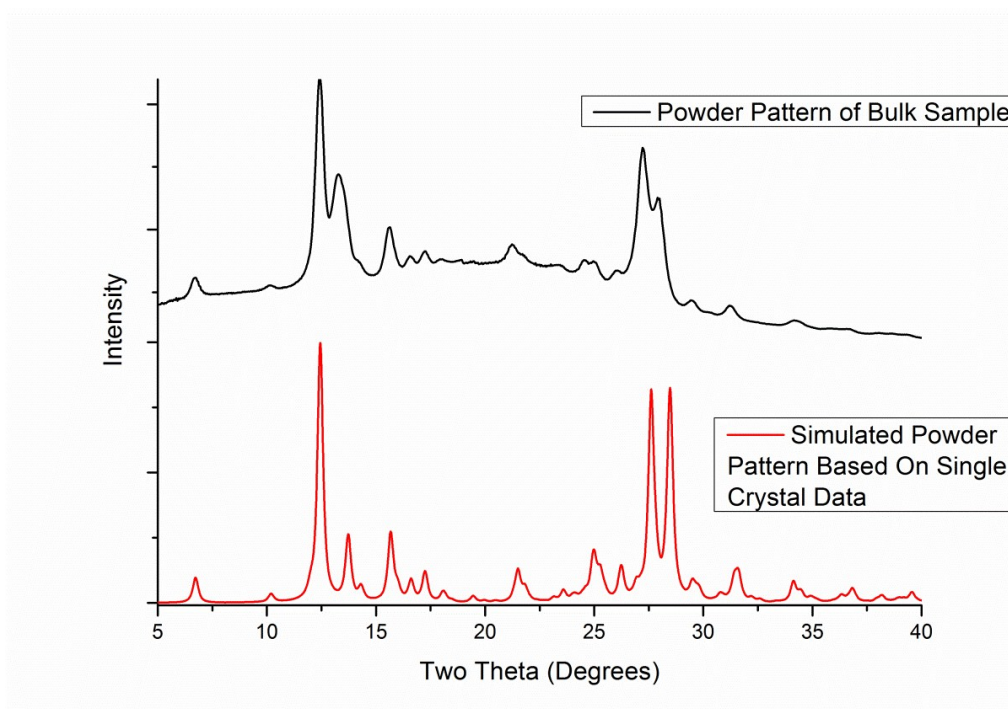


Figure S3.2. Bulk powder pattern and the simulated powder pattern for [(2)TCNQ]. Data collected on an Oxford Diffraction SuperNova Diffractometer at 210 K.

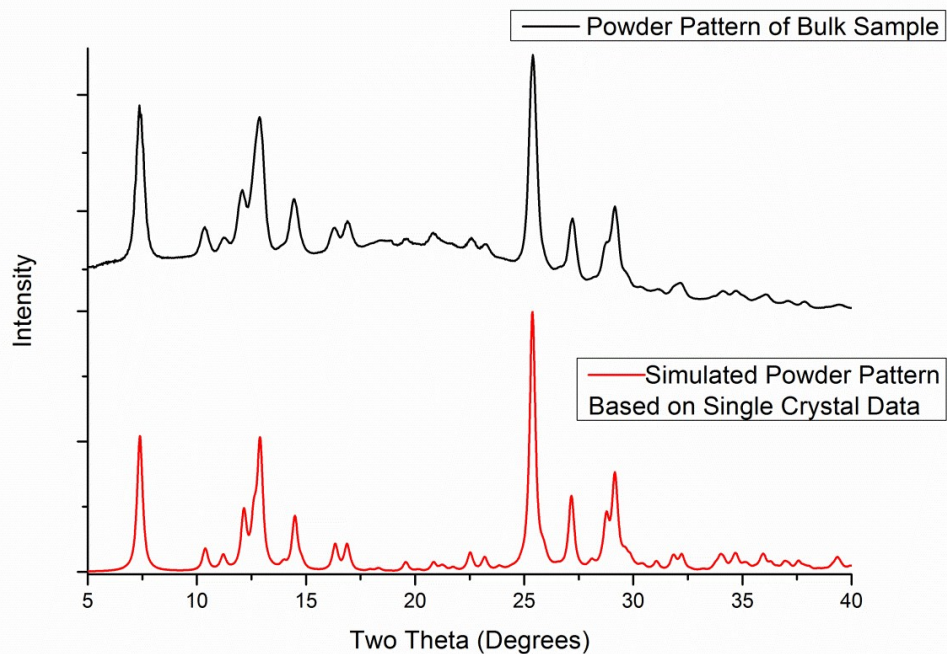


Figure S3.3. Bulk powder pattern and the simulated powder pattern for [(2)F₄TCNQ]. Data collected on an Oxford Diffraction SuperNova Diffractometer at 130 K.

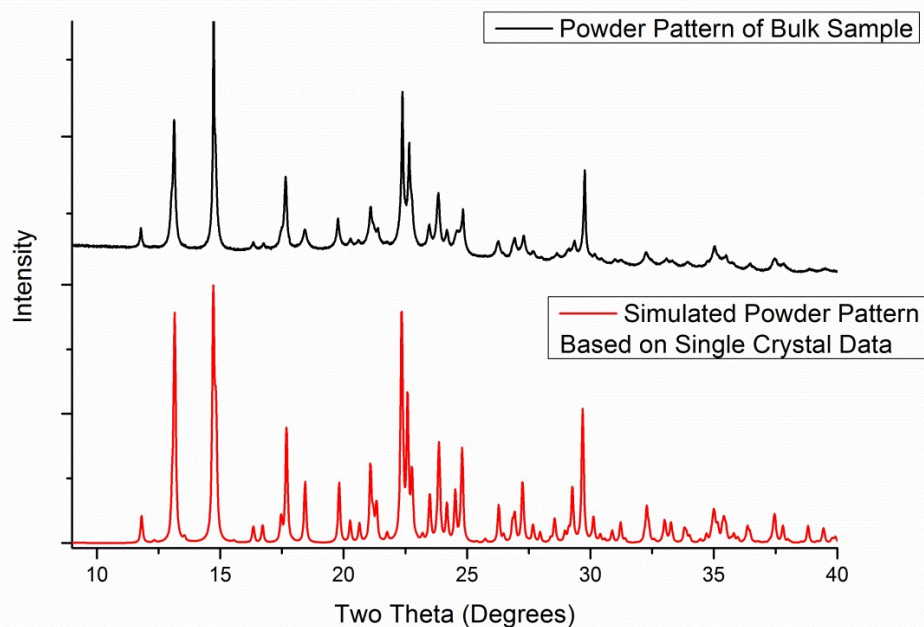


Figure S3.4. Bulk powder pattern and the simulated powder pattern for [(3)TCNQ]. Data collected on the Powder Diffraction Beamline at the Australian Synchrotron at 130 K.

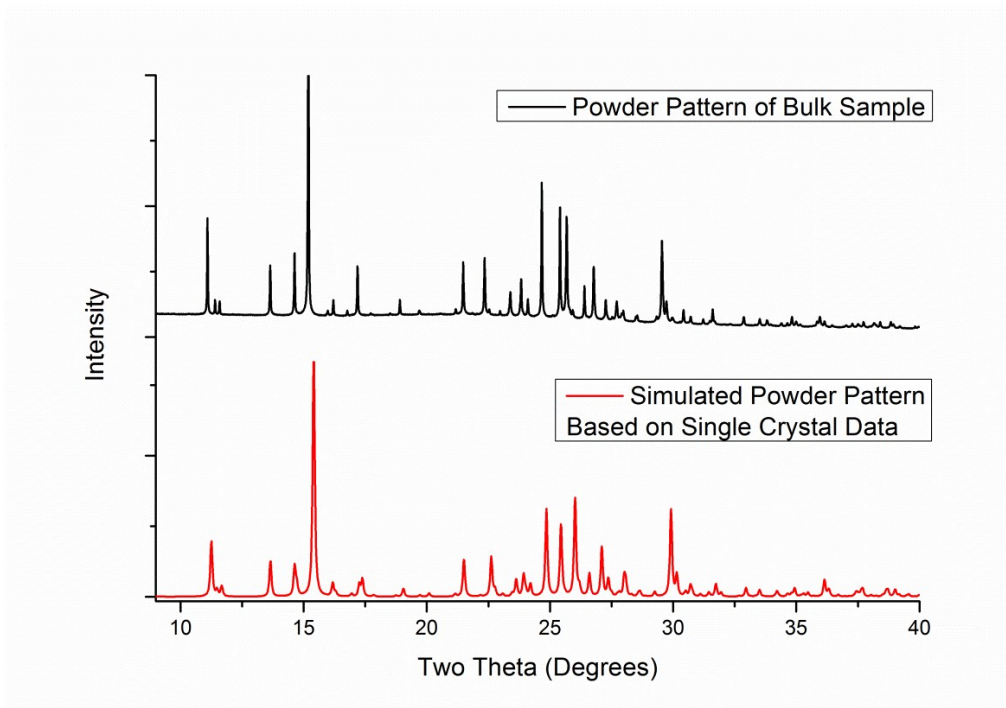


Figure S3.5. Bulk powder pattern and the simulated powder pattern for [(4)TCNQ₂]. Data collected on the Powder Diffraction Beamline at the Australian Synchrotron at RT.

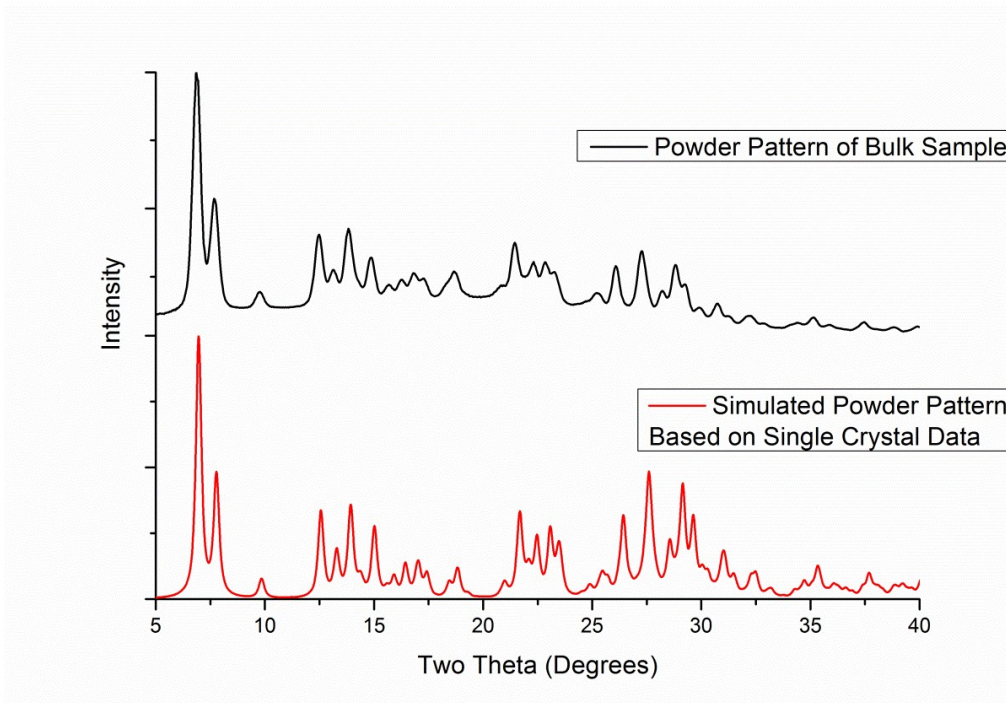


Figure S3.6. Bulk powder pattern and the simulated powder pattern for [(5)TCNQ]. Data collected on an Oxford Diffraction SuperNova Diffractometer at 273 K.

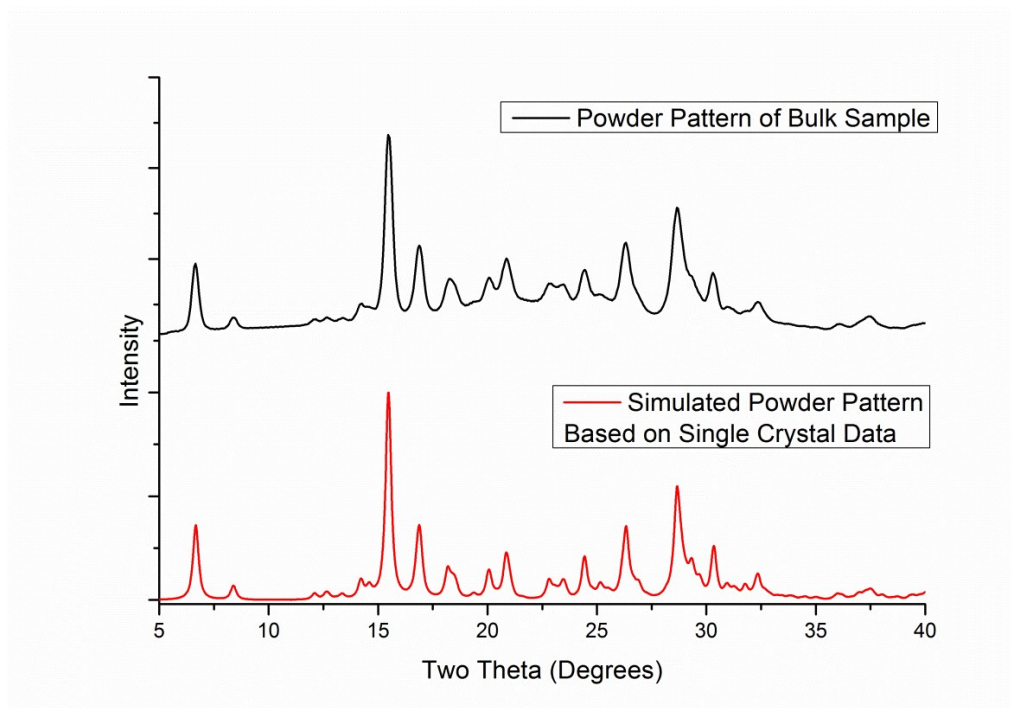


Figure S3.7. Bulk powder pattern and the simulated powder pattern for [(6)TCNQ]. Data collected on an Oxford Diffraction SuperNova Diffractometer at 144 K.

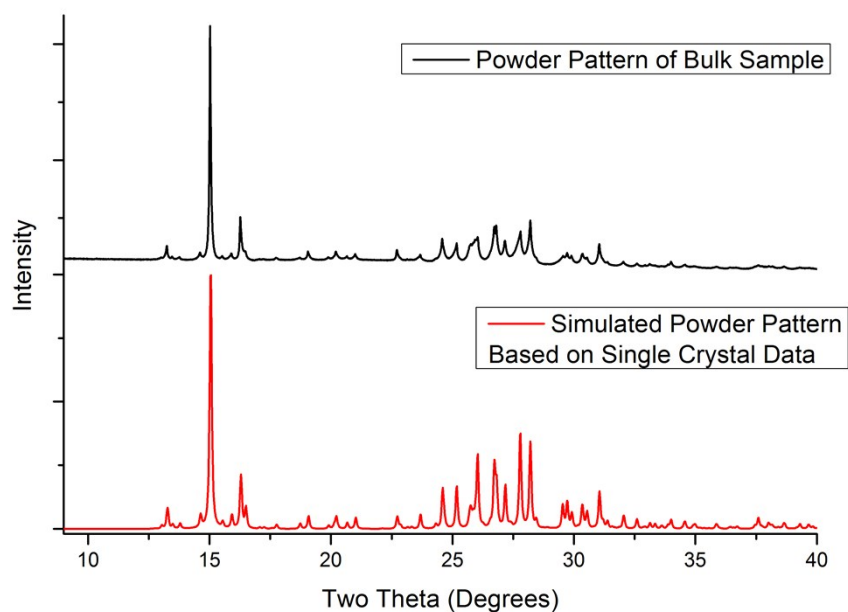


Figure S3.8. Bulk powder pattern and the simulated powder pattern for [(7)TCNQ]. Data collected on the Powder Diffraction Beamline at the Australian Synchrotron at 130 K.

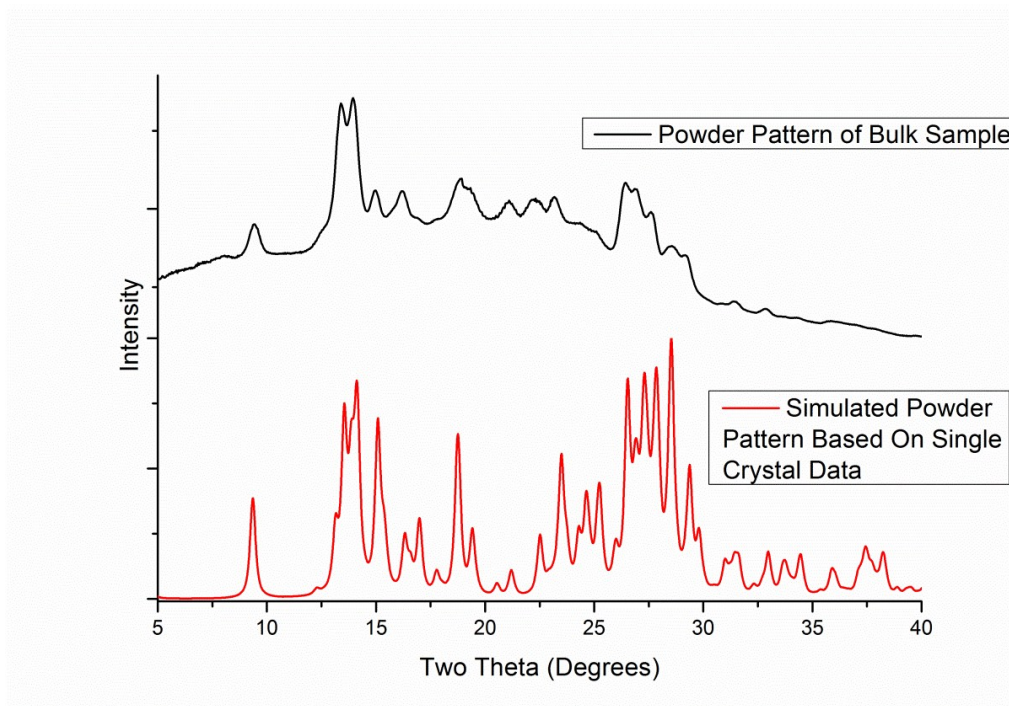


Figure S3.9. Bulk powder pattern and the simulated powder pattern for [(8)TCNQ]. Data collected on an Oxford Diffraction SuperNova Diffractometer at 293 K.

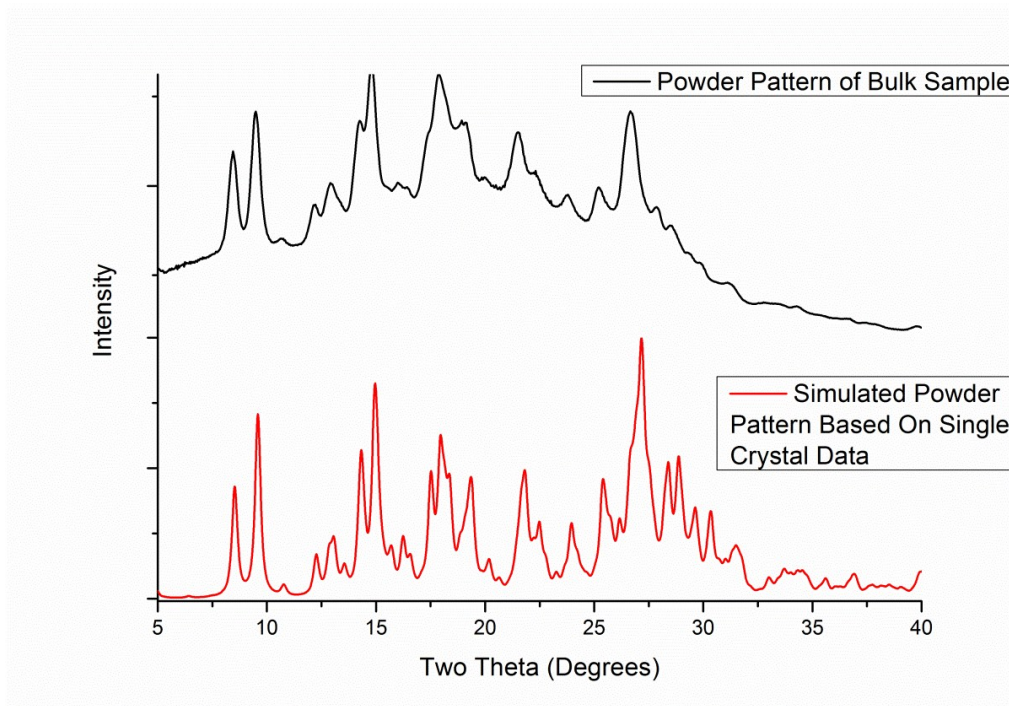


Figure S3.10. Bulk powder pattern and the simulated powder pattern for [(9)TCNQ₂]. Data collected on an Oxford Diffraction SuperNova Diffractometer at 143 K.

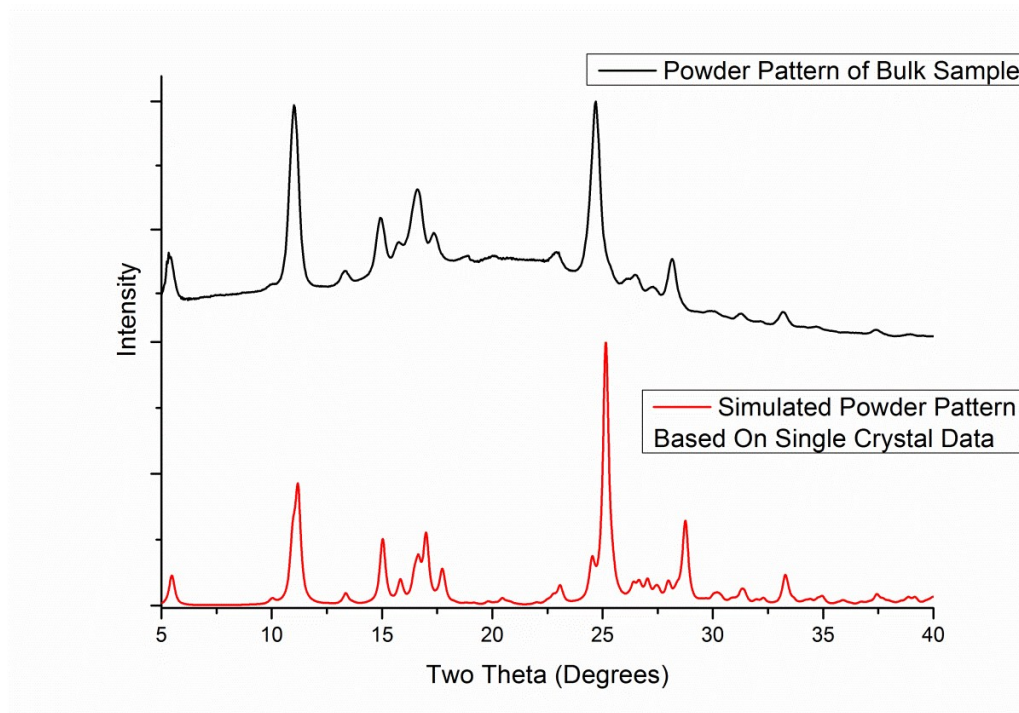


Figure S3.11. Bulk powder pattern and the simulated powder pattern for [(10)F₄TCNQ]. Data collected on an Oxford Diffraction SuperNova Diffractometer at 143 K.

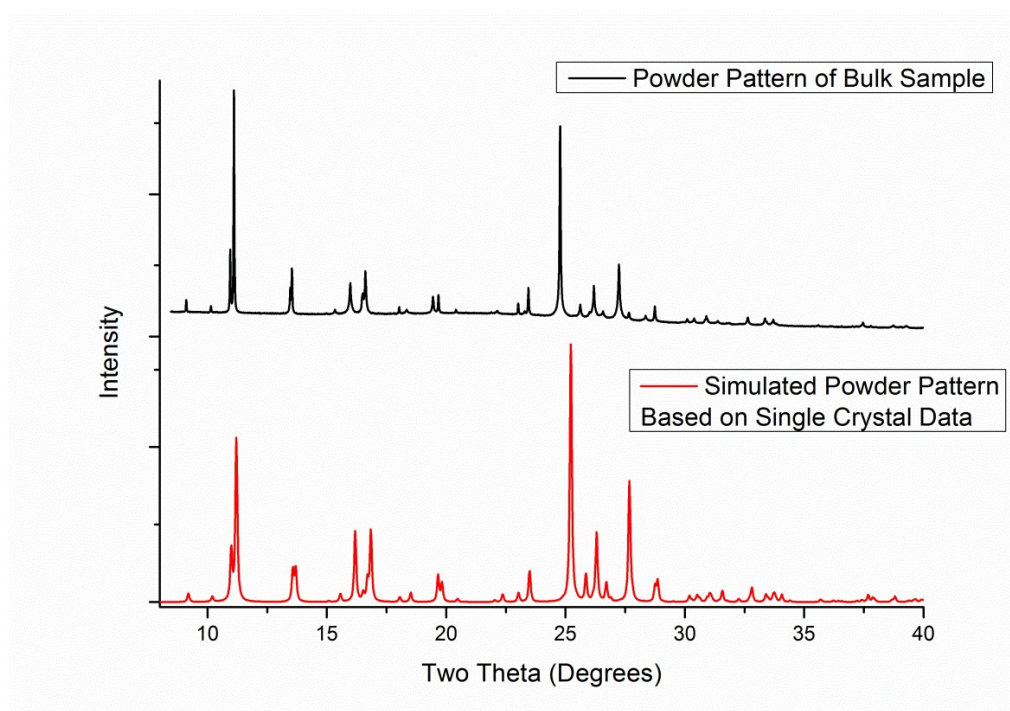


Figure S3.12. Bulk powder pattern and the simulated powder pattern for [(10)TCNQ]. Data collected on the Powder Diffraction Beamline at the Australian Synchrotron at RT.

S4 – EPR Spectra

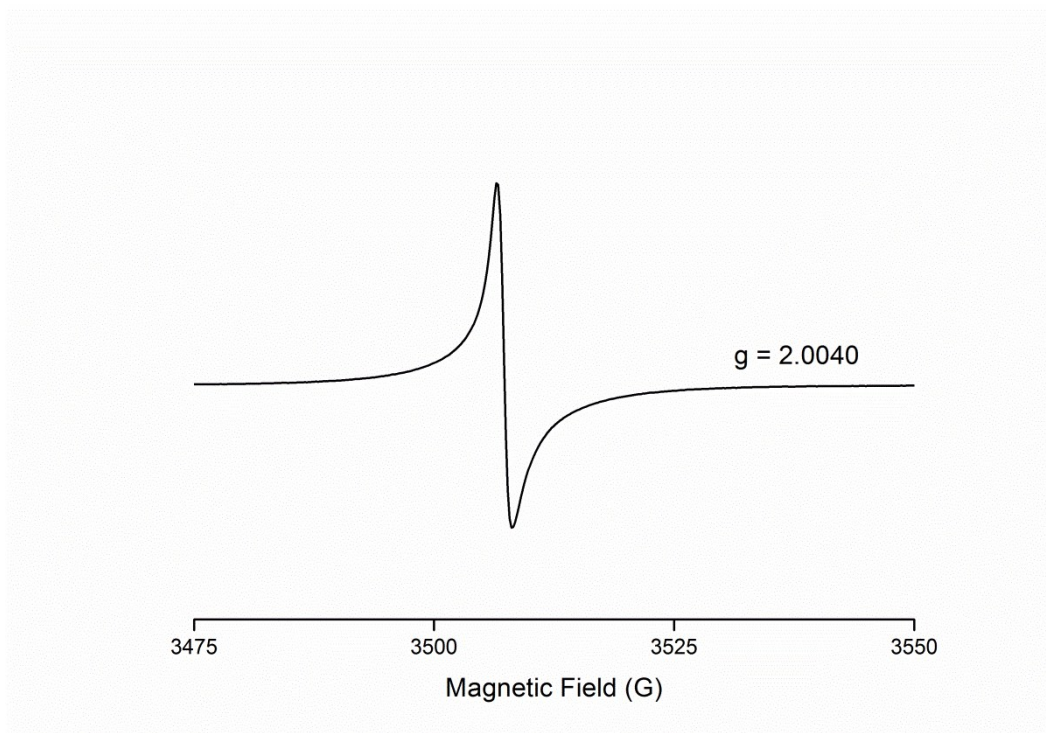


Figure S4.1. EPR spectrum of [(1)TCNQ].

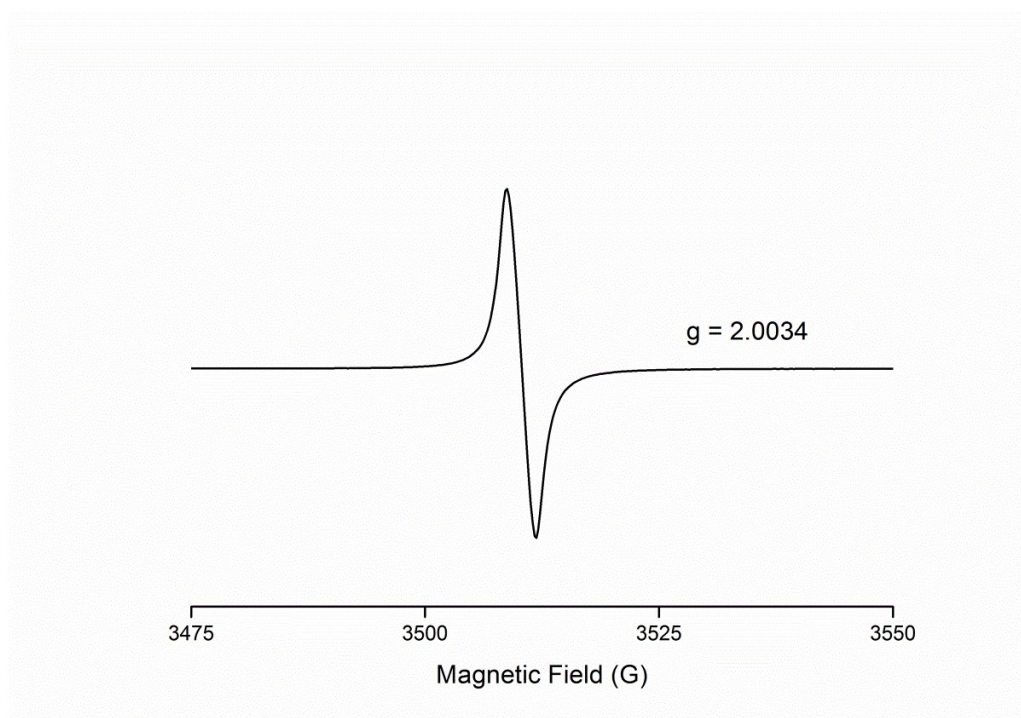


Figure S4.2. EPR spectrum of [(2)TCNQ].

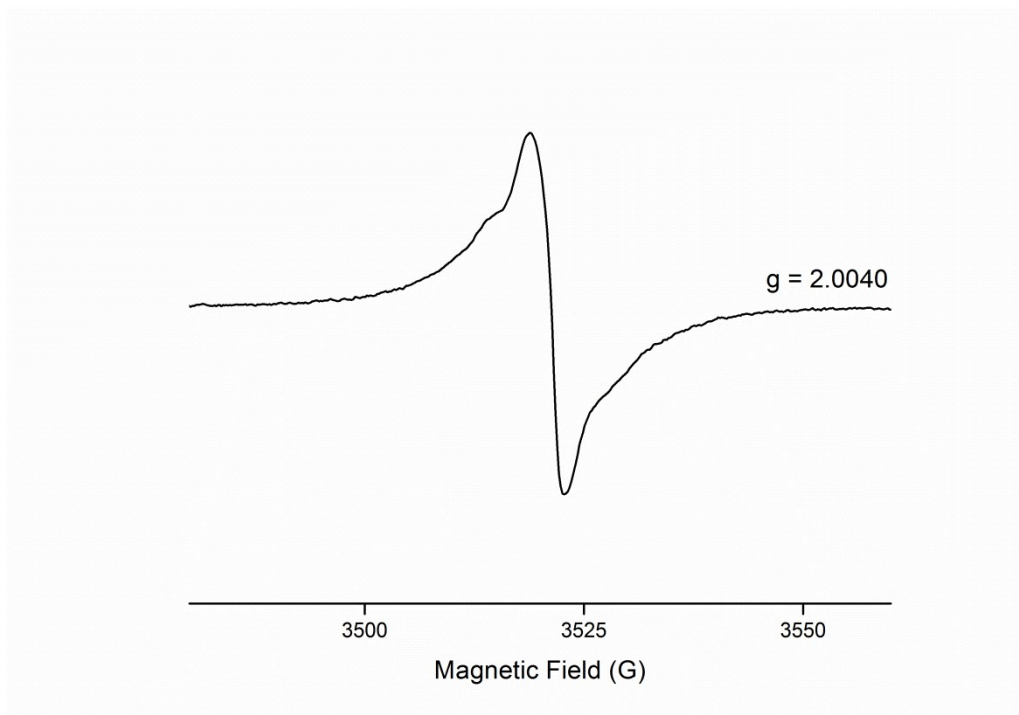


Figure S4.3. EPR spectrum of [(2)F₄TCNQ].

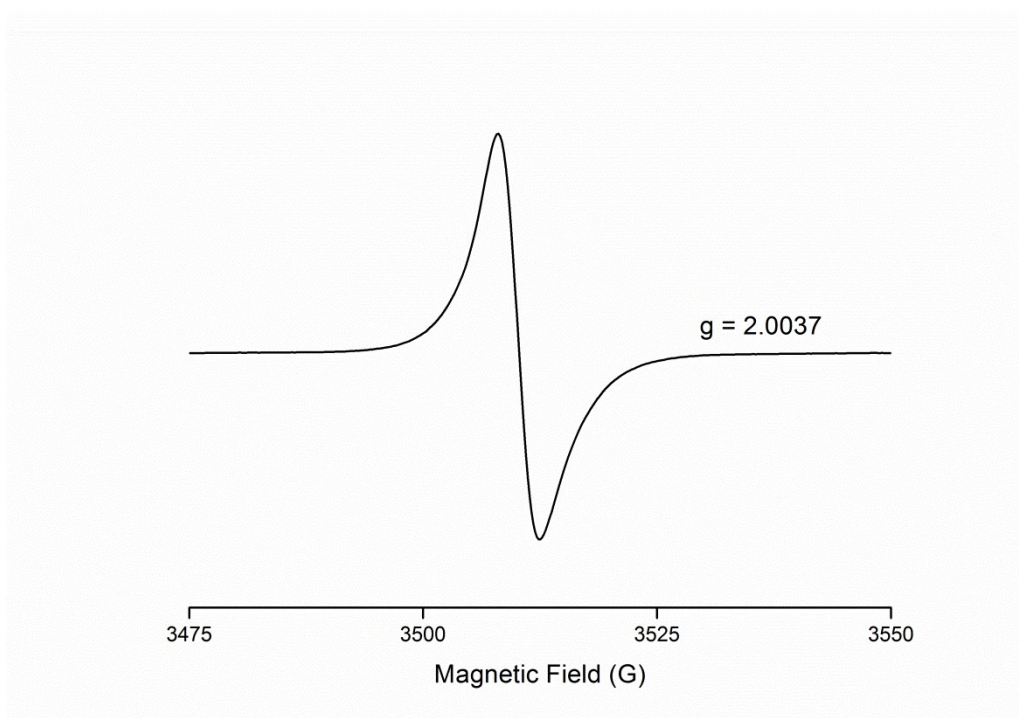


Figure S4.4. EPR spectrum of [(3)TCNQ].

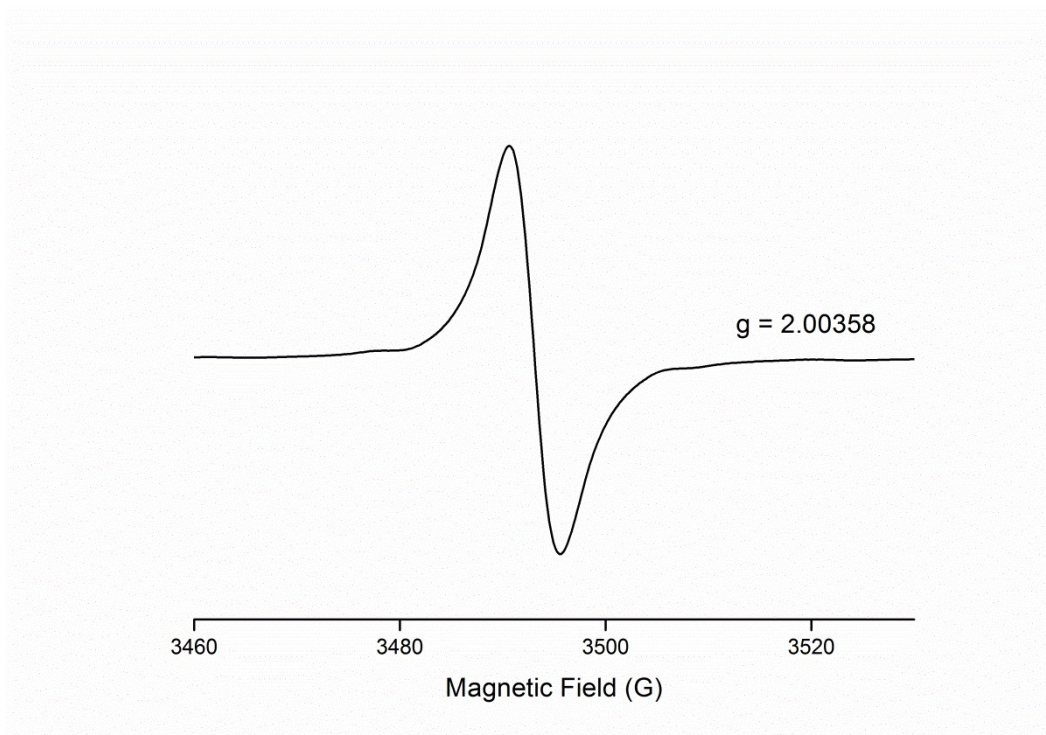


Figure S4.5. EPR spectrum of [(4)TCNQ₂].

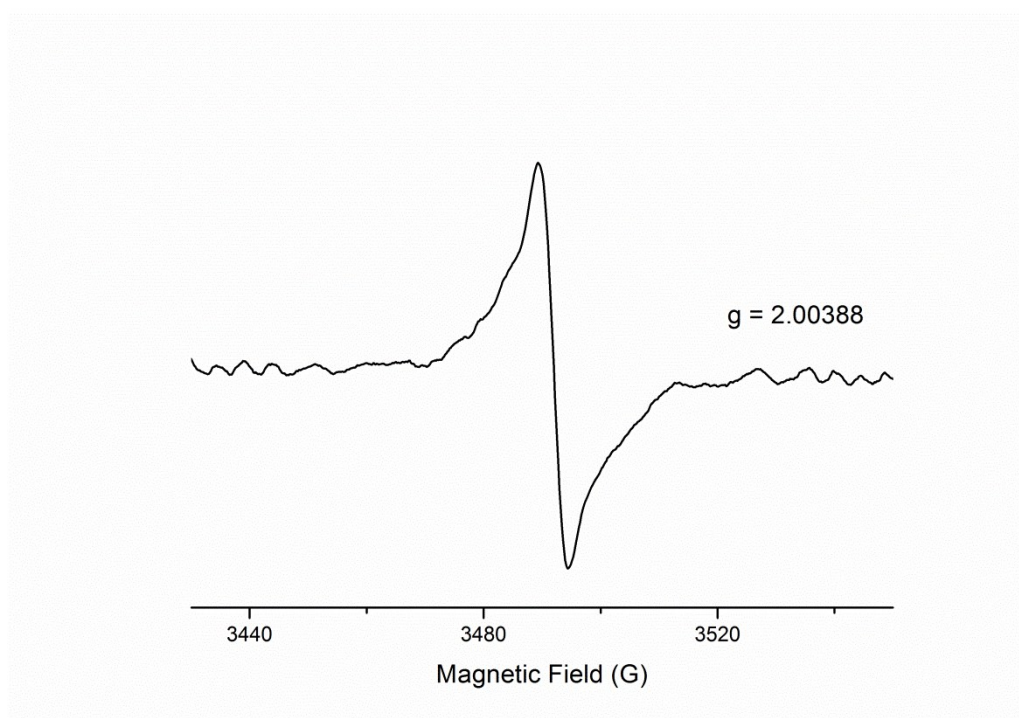


Figure S4.6. EPR spectrum of [(5)TCNQ].

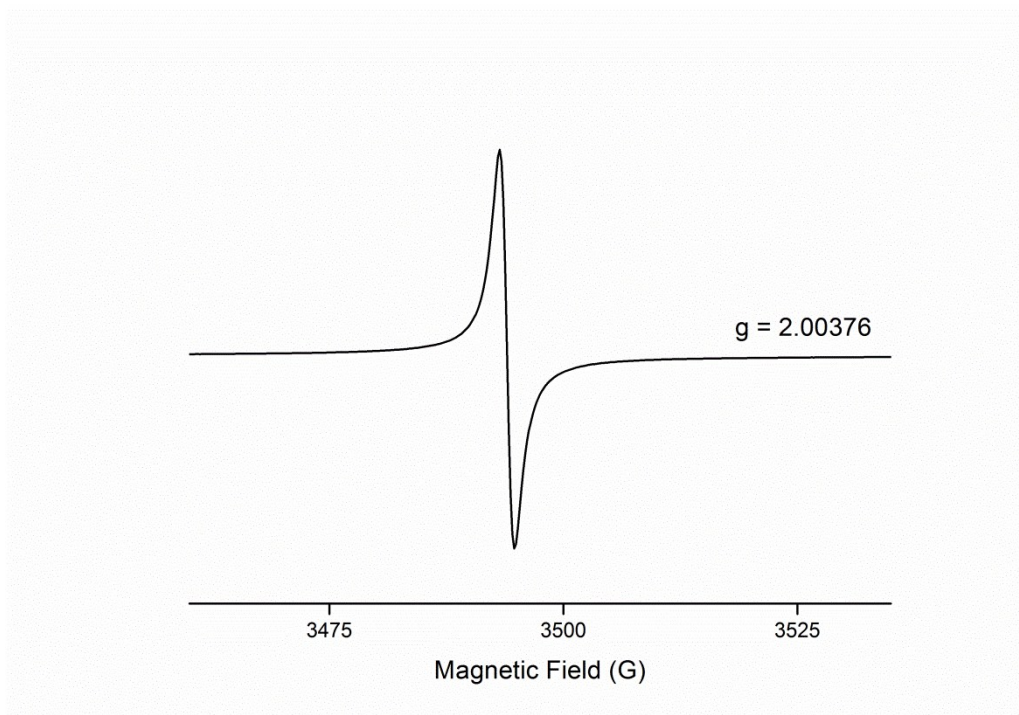


Figure S4.7. EPR spectrum of [(6)TCNQ].

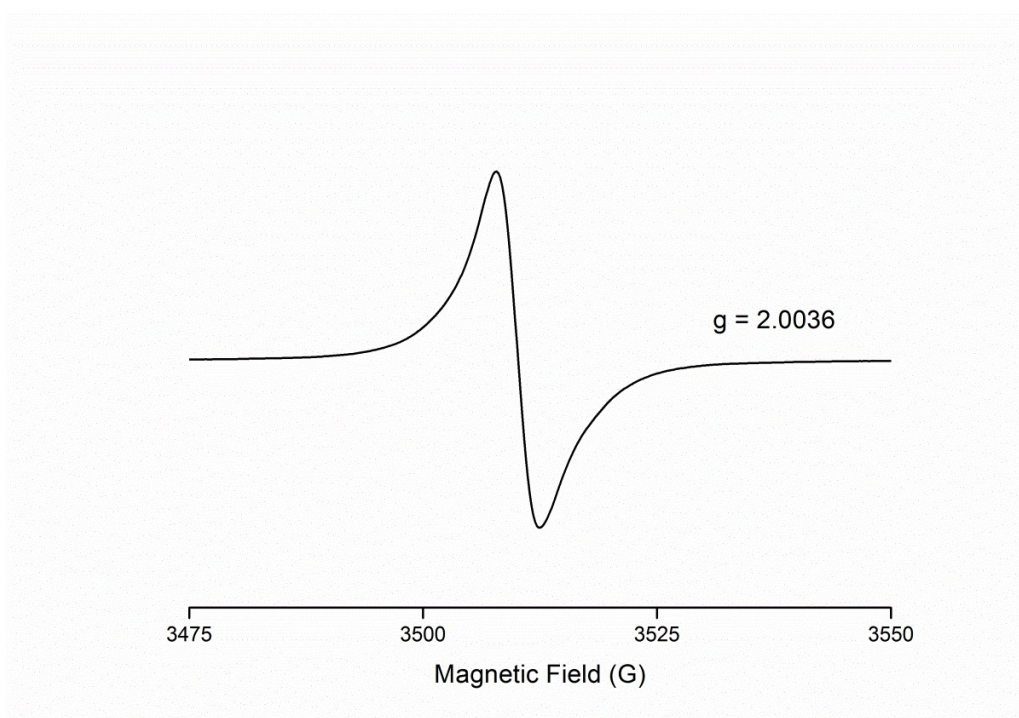


Figure S4.8. EPR spectrum of [(7)TCNQ].

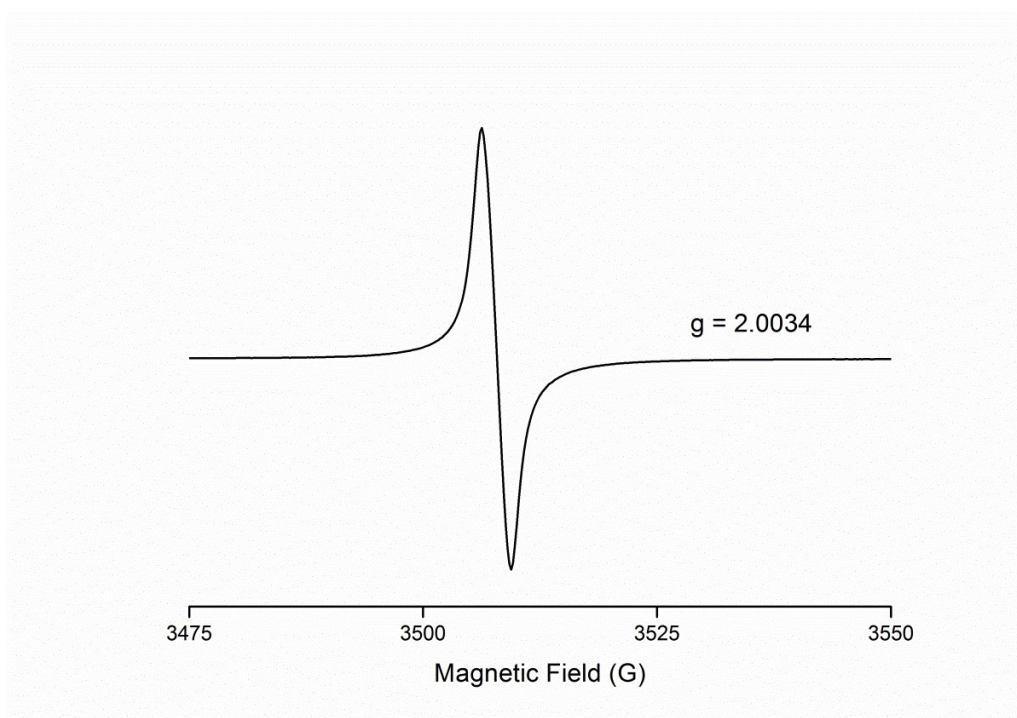


Figure S4.9. EPR spectrum of [(8)TCNQ].

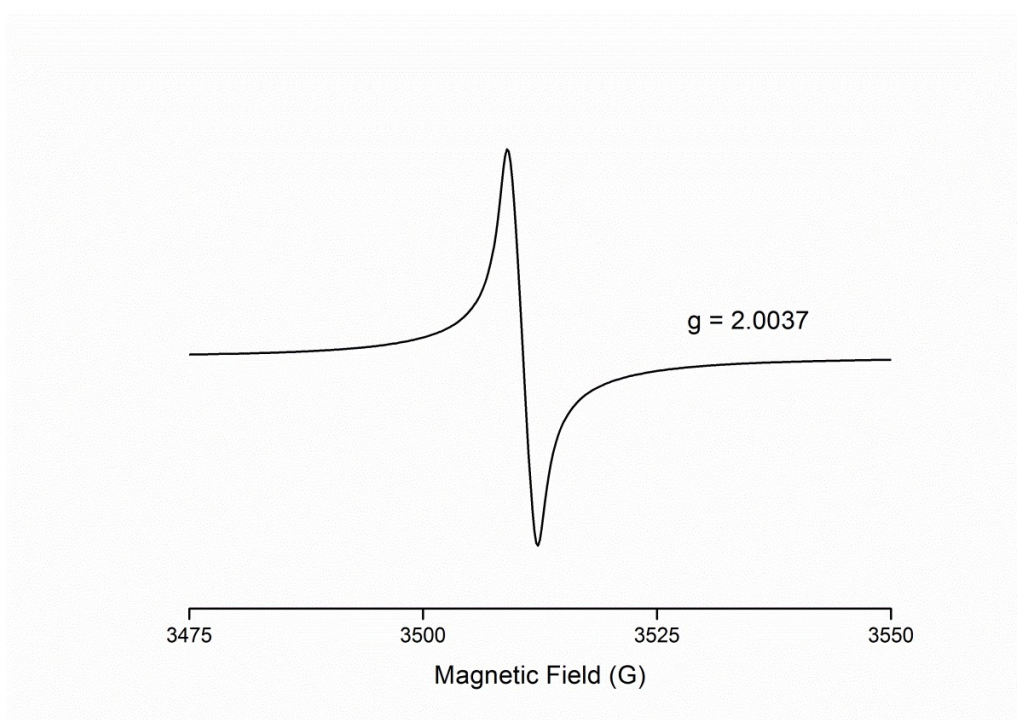


Figure S4.10. EPR spectrum of [(9)TCNQ₂].

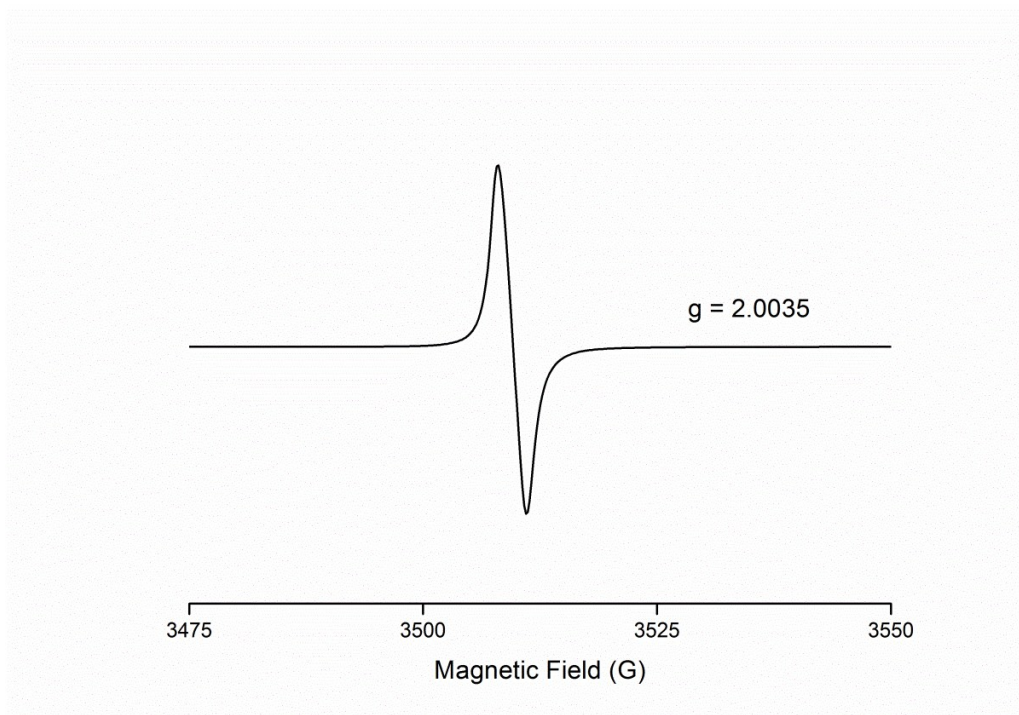


Figure S4.11. EPR spectrum of [(10)TCNQ].

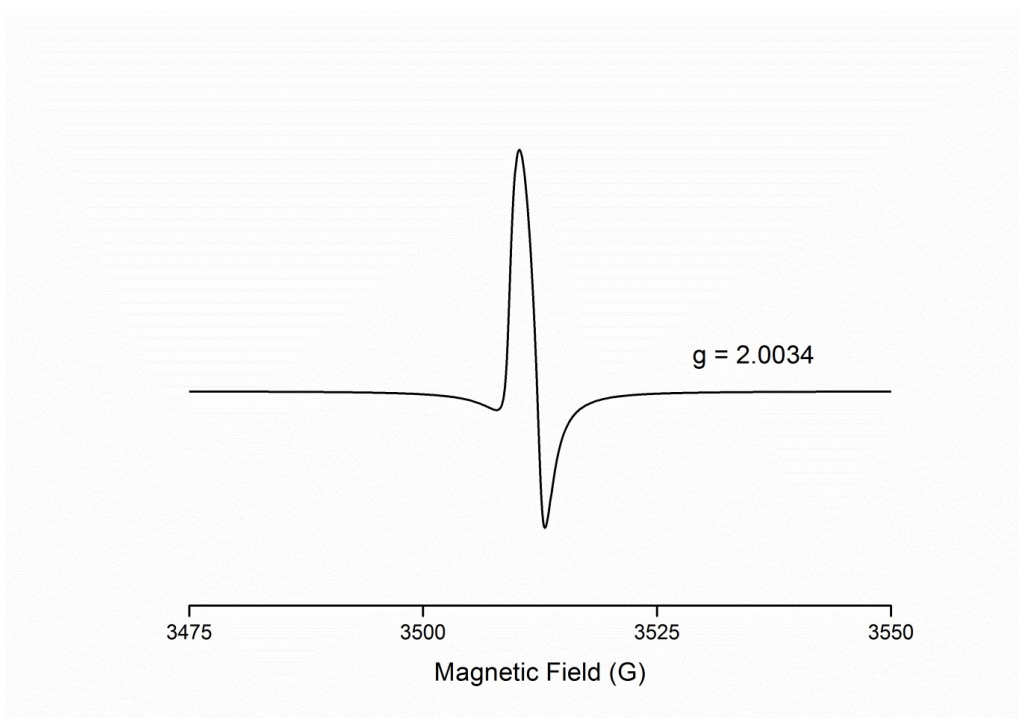


Figure S4.12. EPR spectrum of [(10)F₄TCNQ].

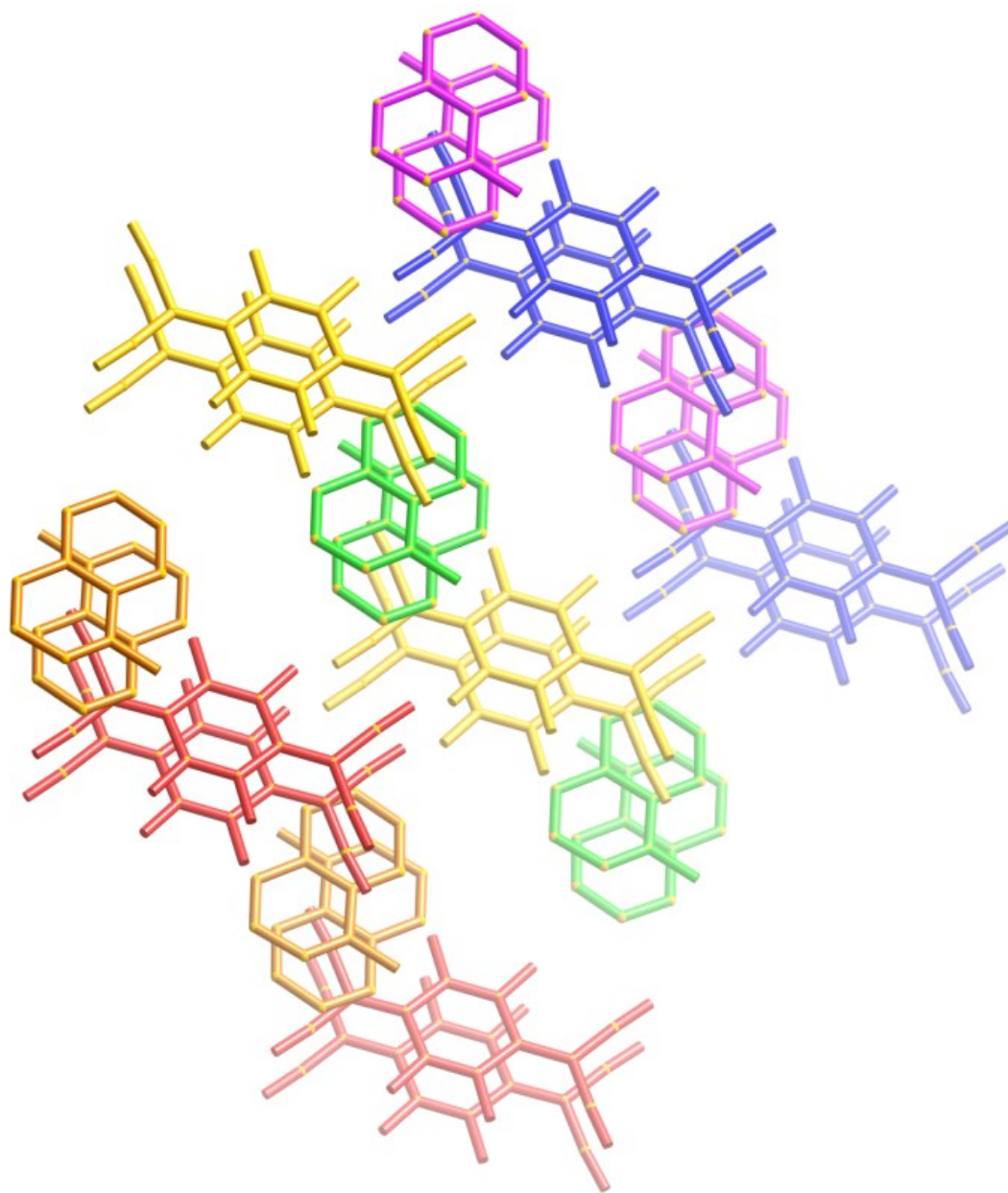


Figure S5.1. Stick representation of $[(2)F_4TCNQ]$ showing the “staircase” formed by the “stepped” face-to-face interactions.

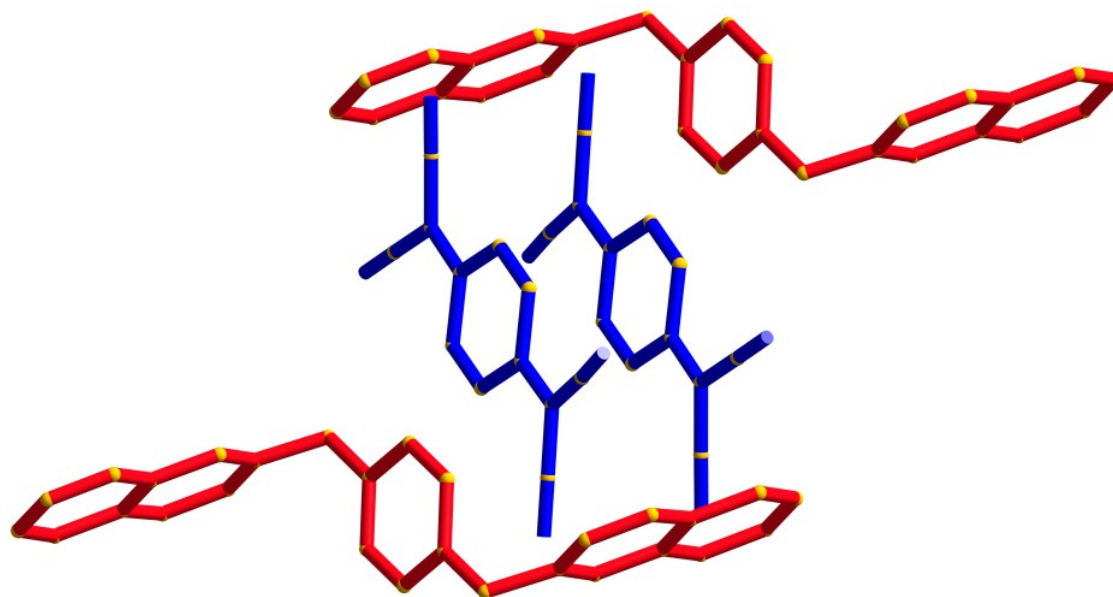


Figure S5.2. Stick representations of $[(4)TCNQ_2]$ viewed side on to the stacking direction showing the interaction between the $-C(CN)_2$ moieties of the TCNQ units and the aromatic faces of (4). The TCNQ units are shown in blue and the cations are shown in red.

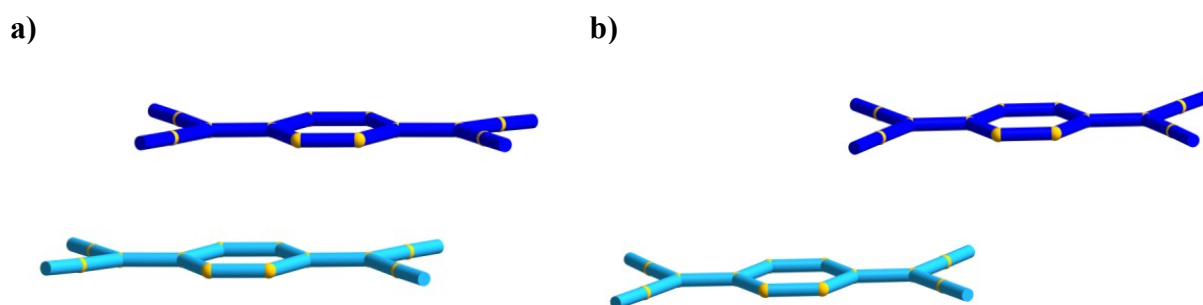
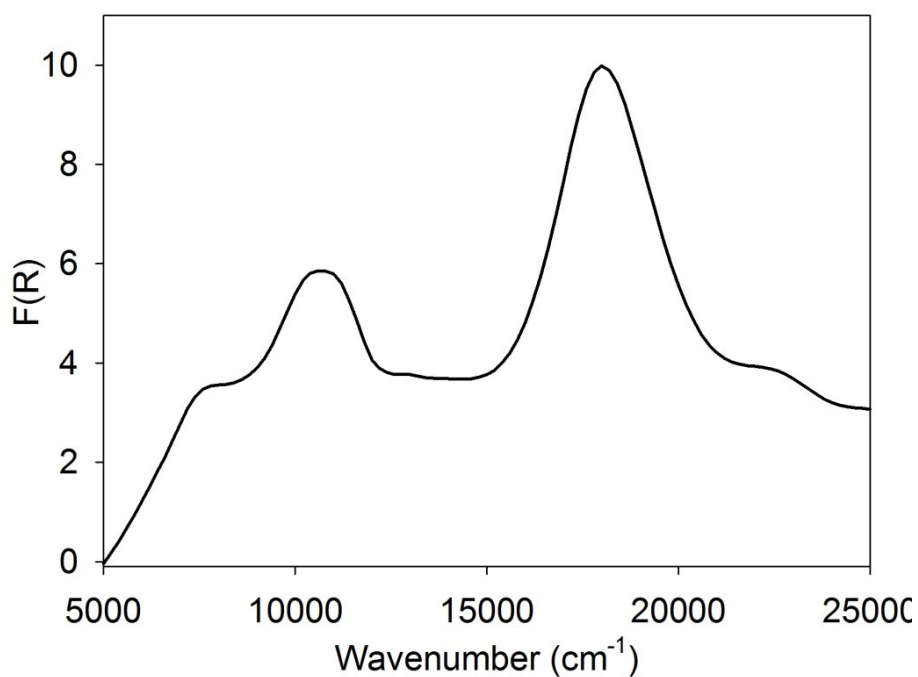


Figure S5.3. Stick representations of the TCNQ dimers showing the longitudinal offsets between the dimer partners (blue and light blue) for **a)** a representative dimer pair for types I & II and **b)** a representative dimer pair for type III.

**S6 - Supplementary Vis-NIR solid-state diffuse reflectance spectra
and corresponding Tauc plots**

a)



b)

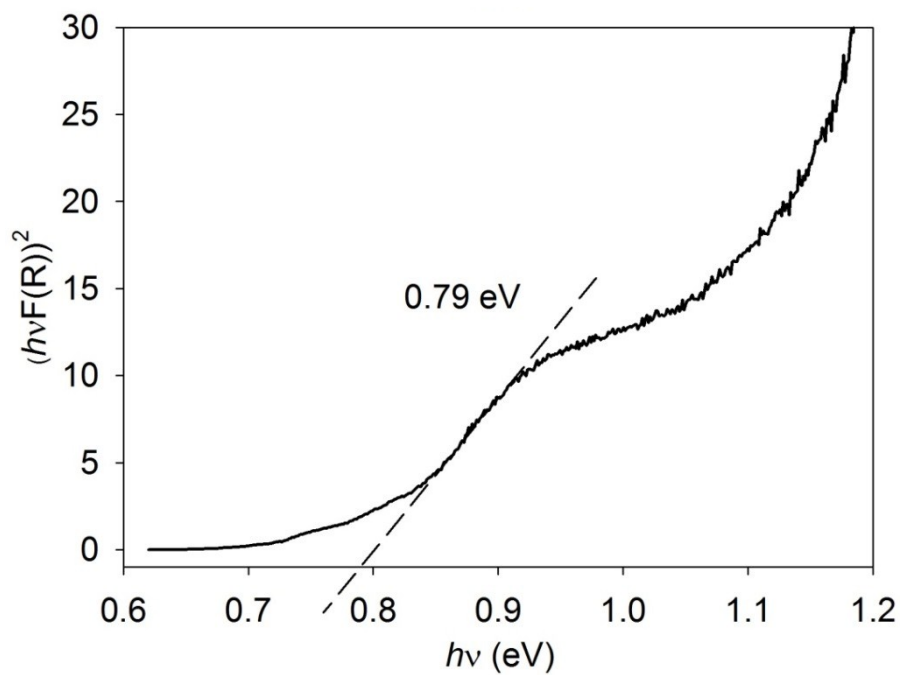
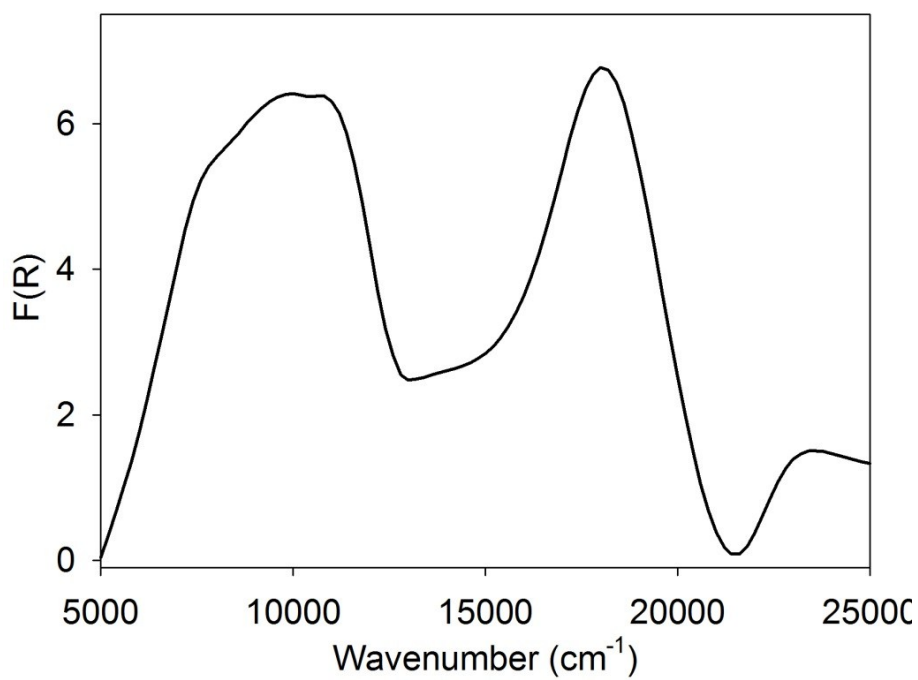


Fig. S6.1 a) The Vis-NIR solid-state diffuse reflectance spectrum of [(1)TCNQ]. **b)** The Tauc plot derived from the spectrum showing the estimation of the optical band gap.

a)



b)

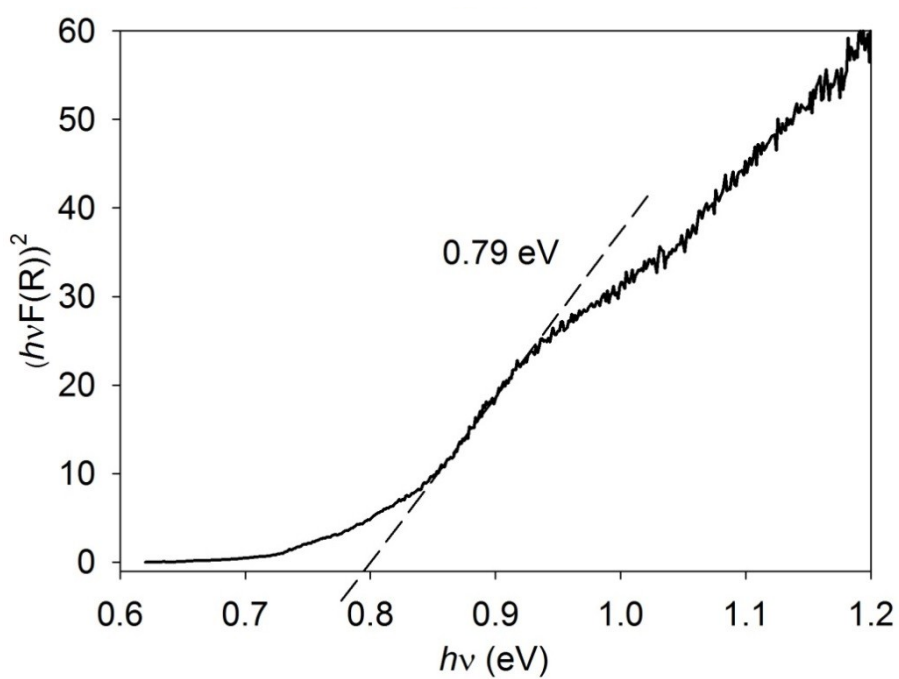
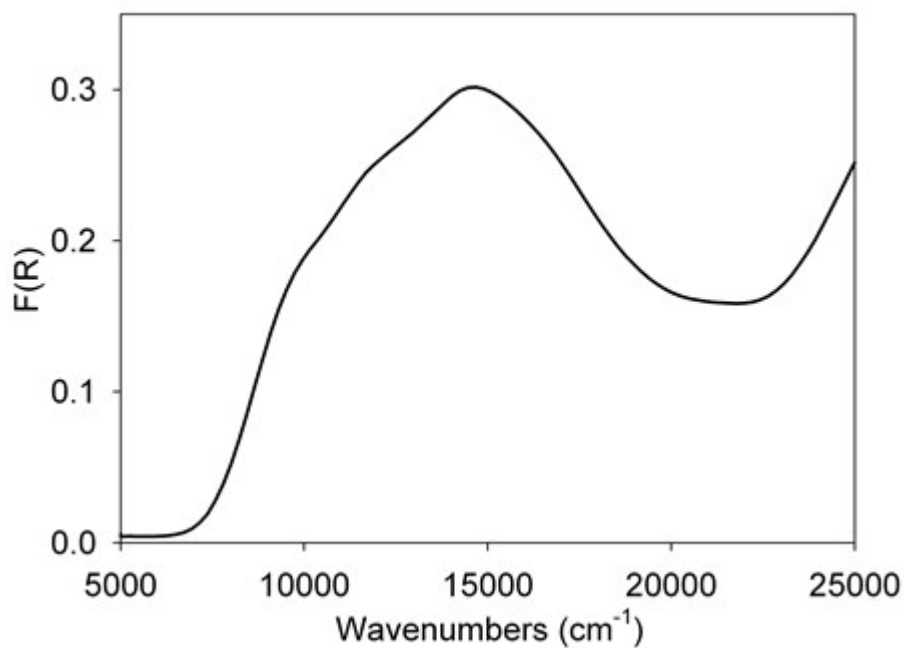


Fig. S6.2 a) The Vis-NIR solid-state diffuse reflectance spectrum of [(2)TCNQ]. b) The Tauc plot derived from the spectrum showing the estimation of the optical band gap.

a)



b)

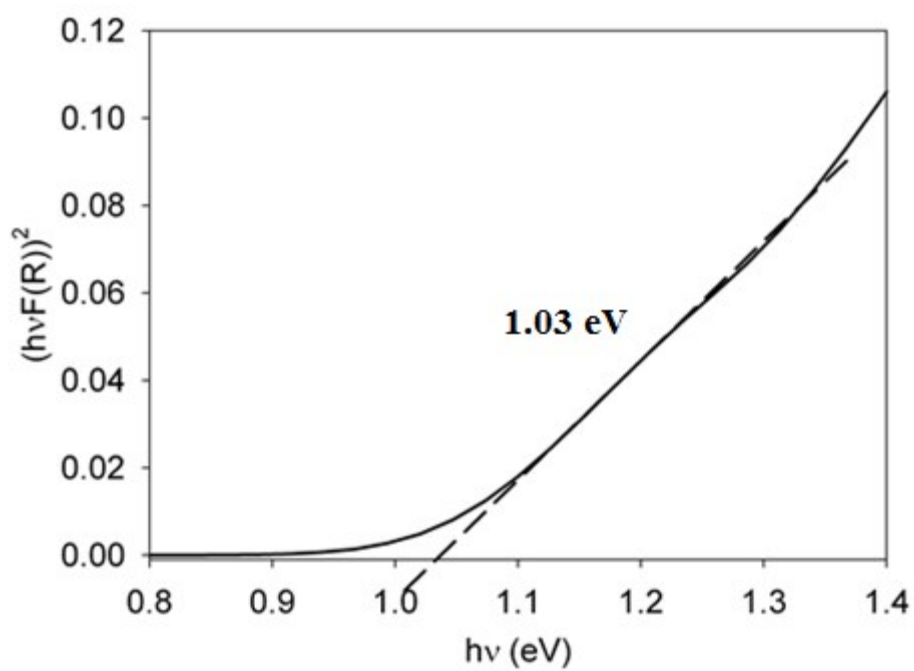
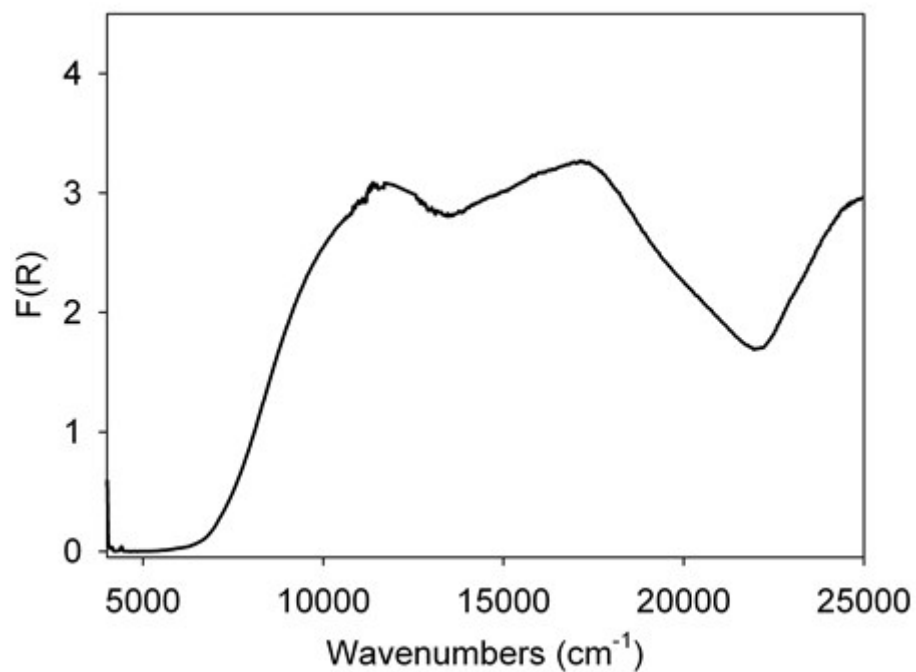


Fig. S6.3 a) The Vis-NIR solid-state diffuse reflectance spectrum of $[(2)F_4TCNQ]$. b) The Tauc plot derived from the spectrum showing the estimation of the optical band gap.

a)



b)

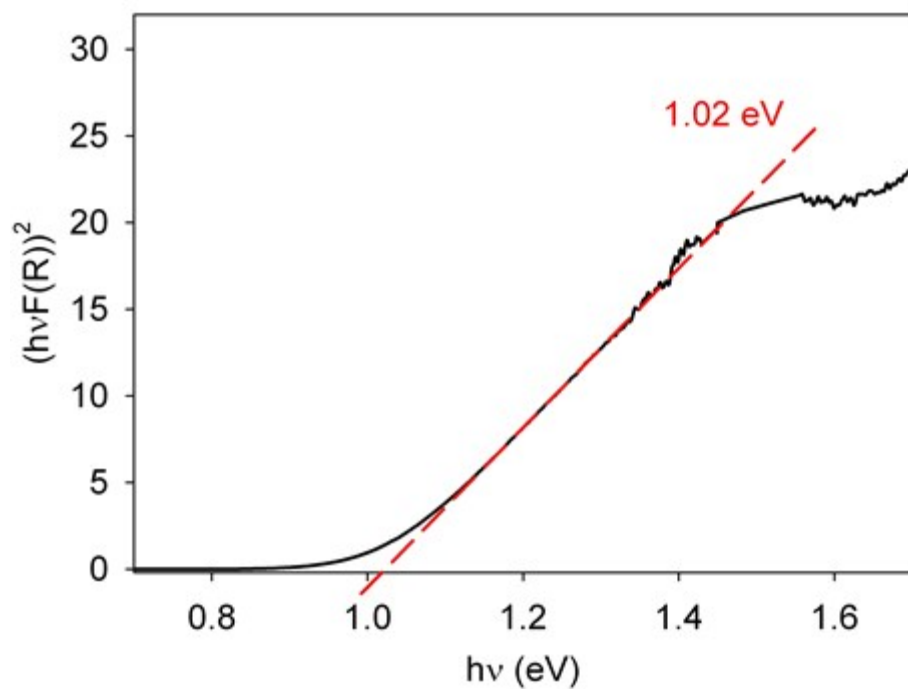
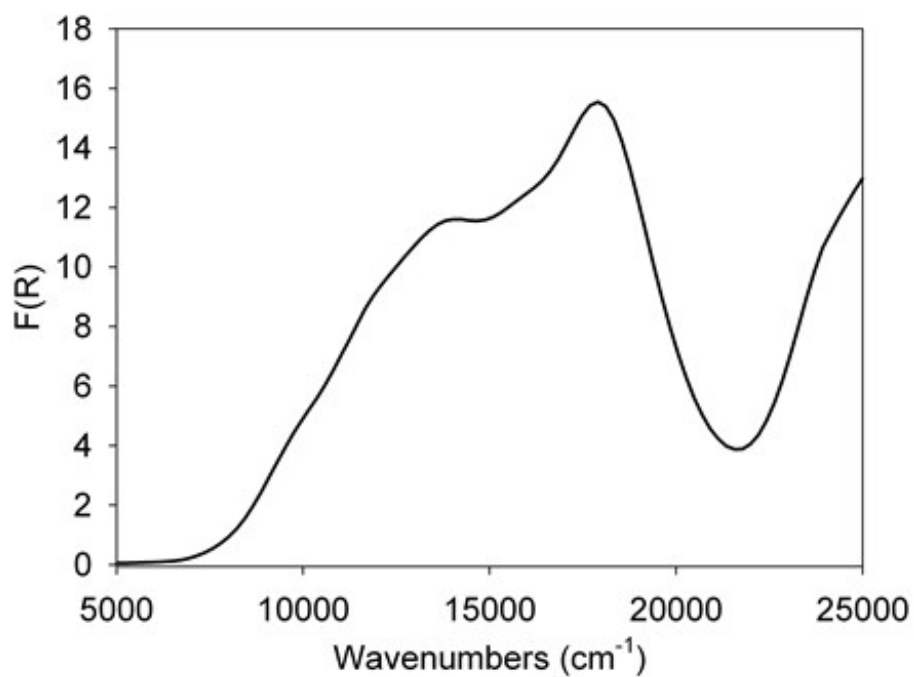


Fig. S6.4 a) The Vis-NIR solid-state diffuse reflectance spectrum of [(3)TCNQ]. b) The Tauc plot derived from the spectrum showing the estimation of the optical band gap.

a)



b)

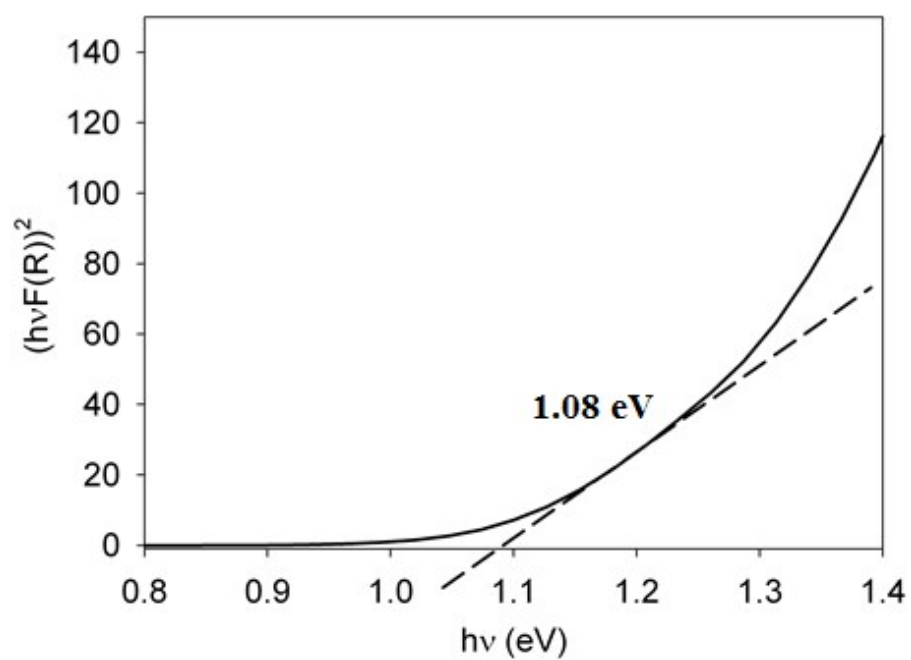
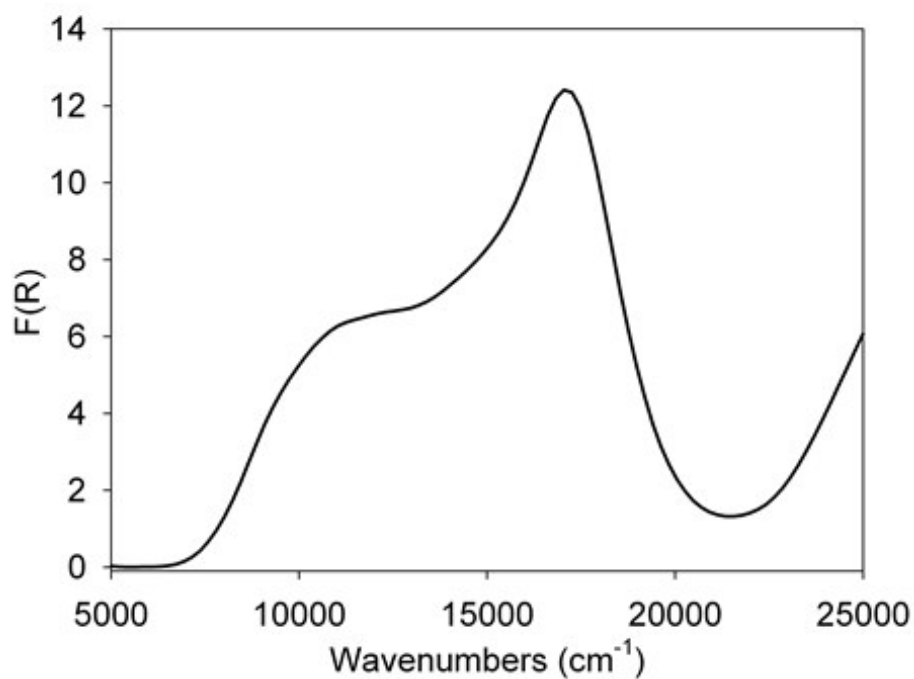


Fig. S6.5 a) The Vis-NIR solid-state diffuse reflectance spectrum of [(4)TCNQ₂]. b) The Tauc plot derived from the spectrum showing the estimation of the optical band gap

a)



b)

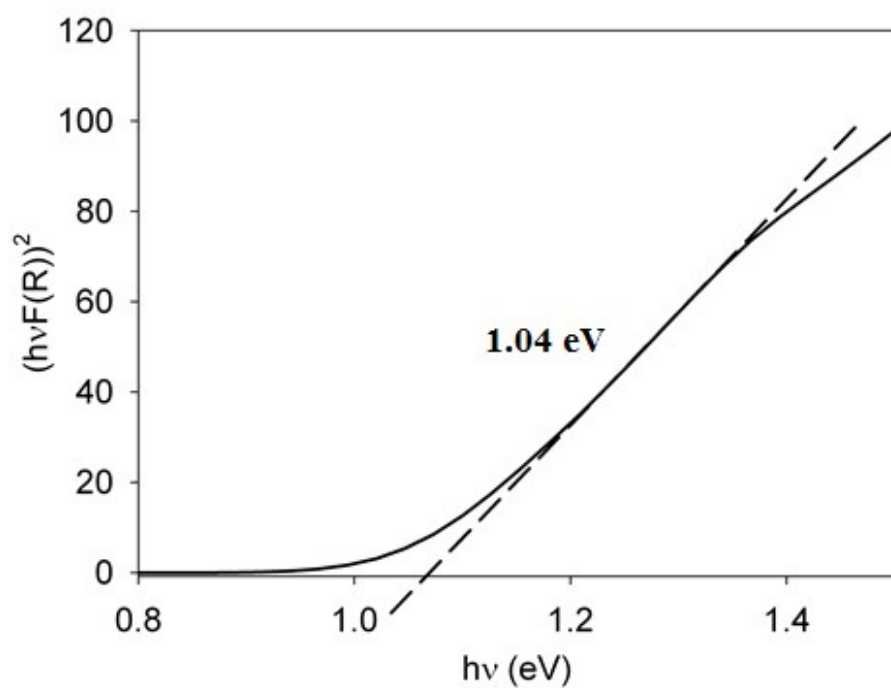
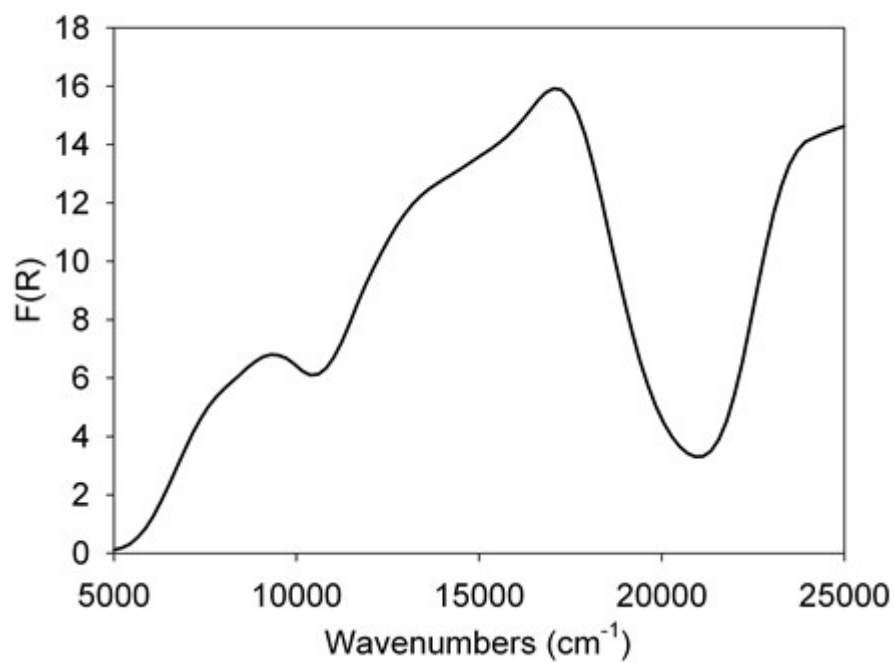


Fig. S6.6 a) The Vis-NIR solid-state diffuse reflectance spectrum of [(5)F₄TCNQ]. b) The Tauc plot derived from the spectrum showing the estimation of the optical band gap.

a)



b)

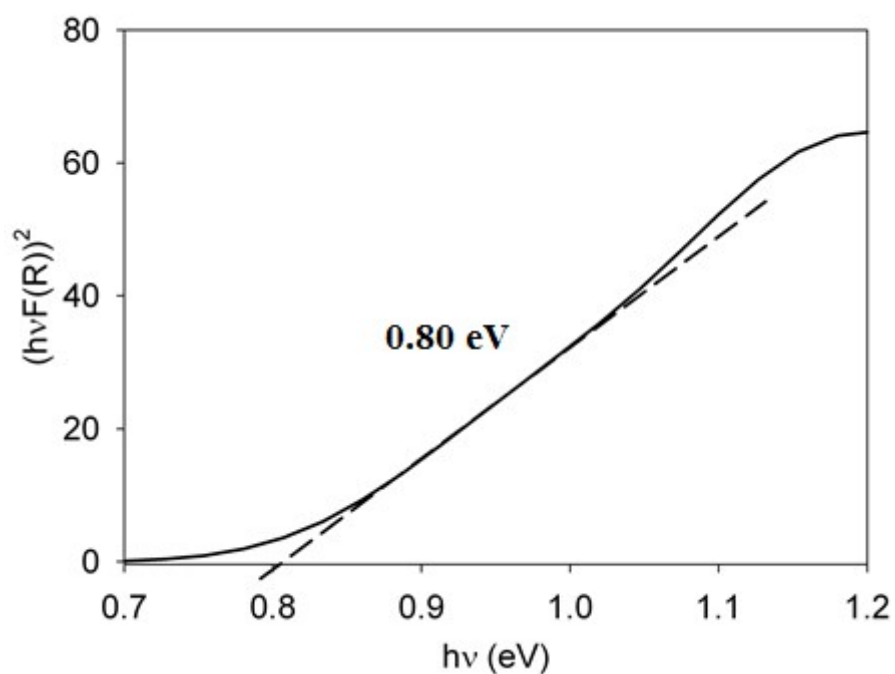
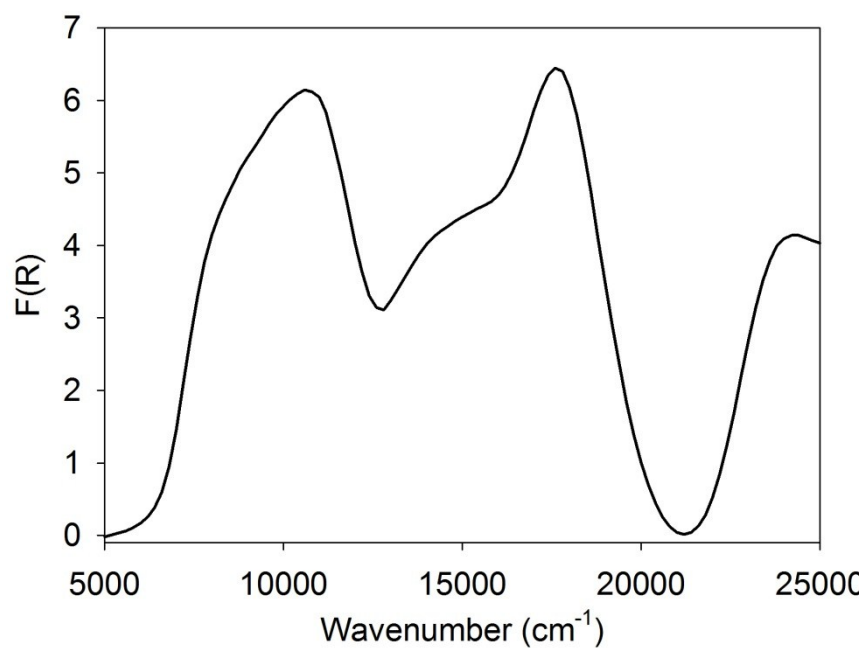


Fig. S6.7 a) The Vis-NIR solid-state diffuse reflectance spectrum of [(6)TCNQ]. b) The Tauc plot derived from the spectrum showing the estimation of the optical band gap.

a)



b)

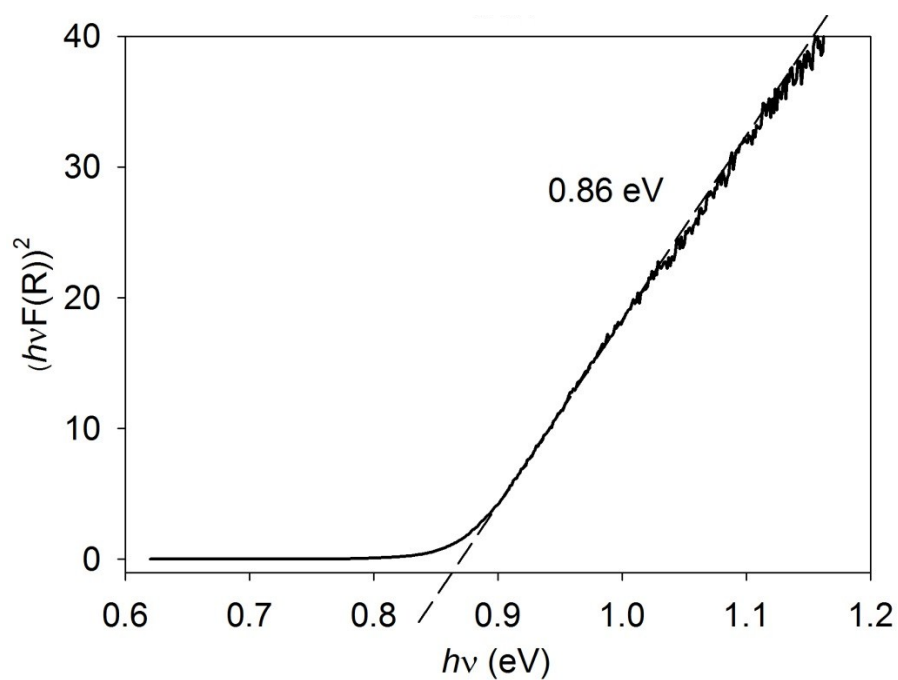
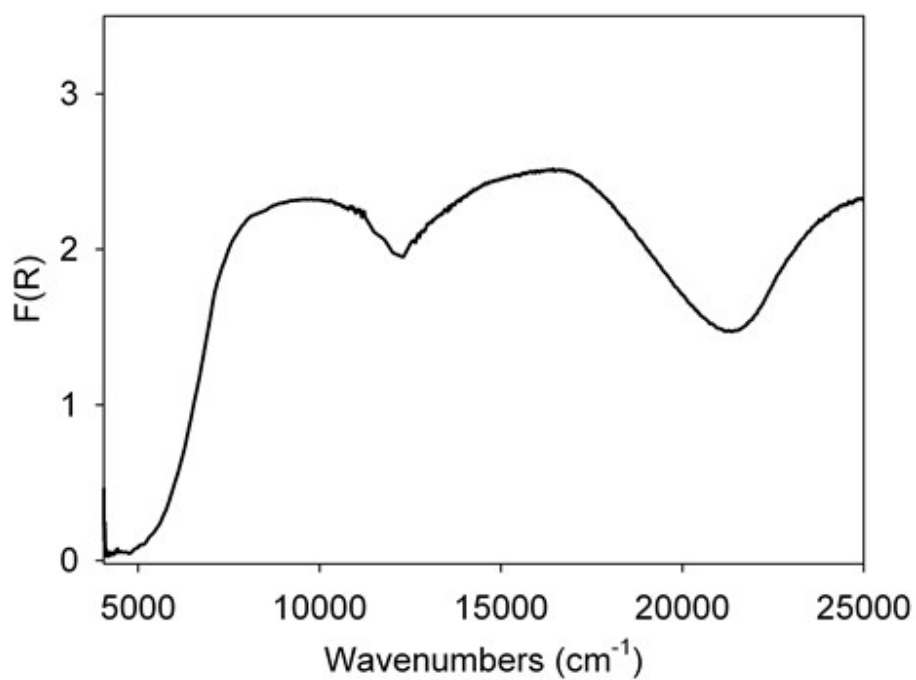


Fig. S6.8 a) The Vis-NIR solid-state diffuse reflectance spectrum of [(7)TCNQ]. b) The Tauc plot derived from the spectrum showing the estimation of the optical band gap.

a)



b)

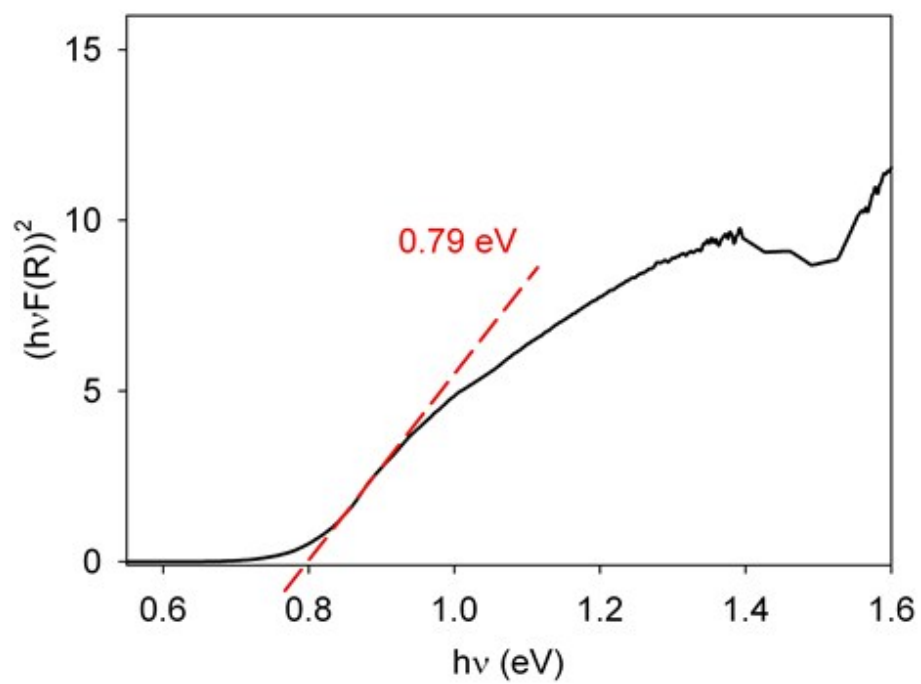
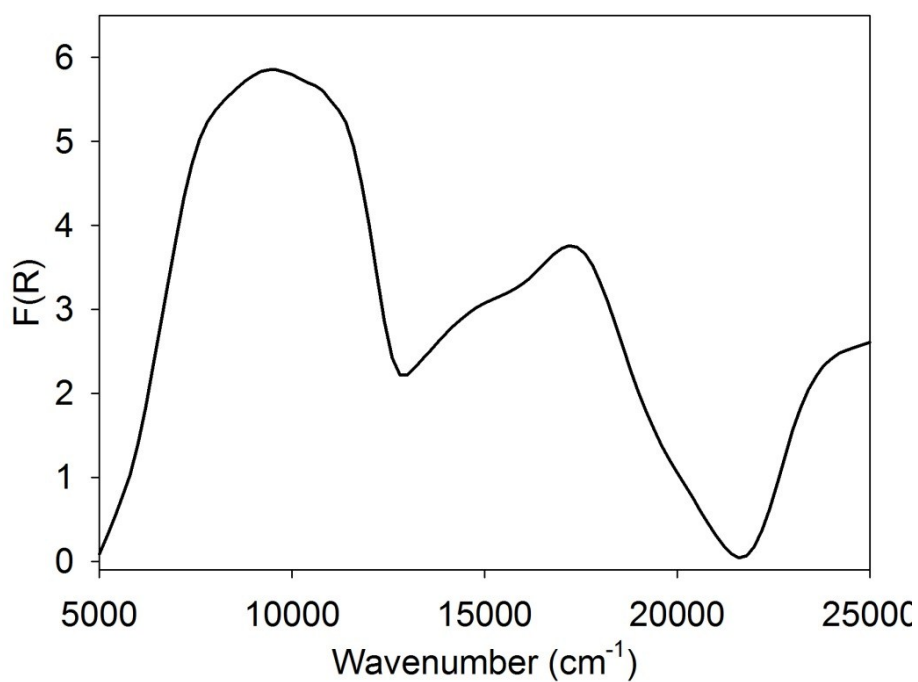


Fig. S6.9 a) The Vis-NIR solid-state diffuse reflectance spectrum of [(8)TCNQ]. b) The Tauc plot derived from the spectrum showing the estimation of the optical band gap.

a)



b)

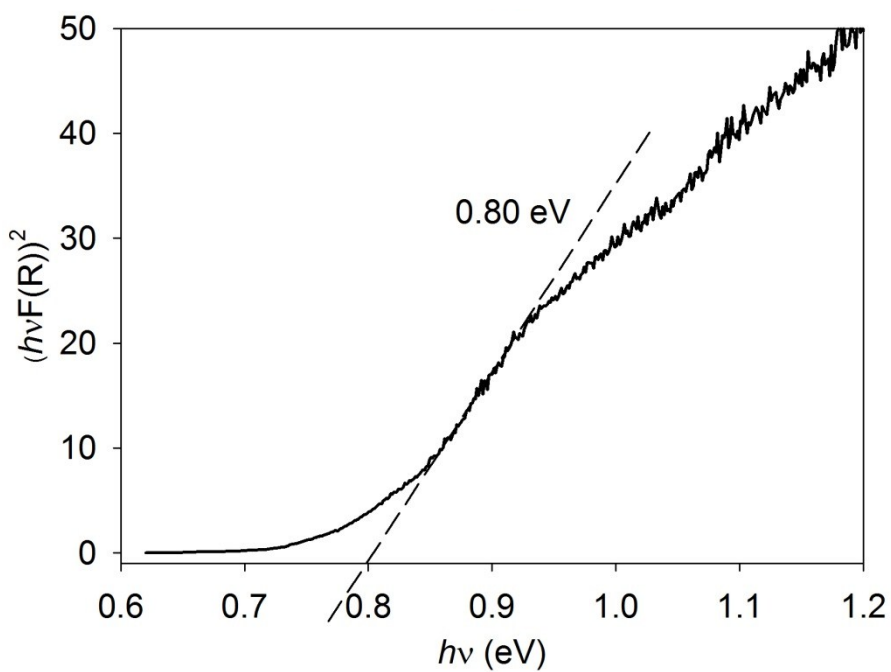
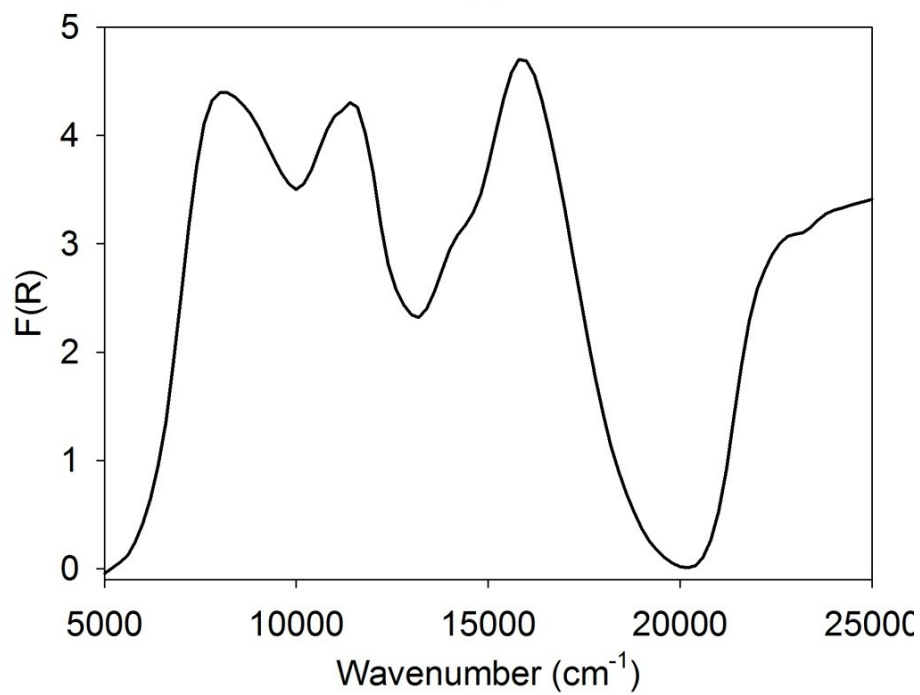


Fig. S6.10 a) The Vis-NIR solid-state diffuse reflectance spectrum of [(9)TCNQ₂]. b) The Tauc plot derived from the spectrum showing the estimation of the optical band gap

a)



b)

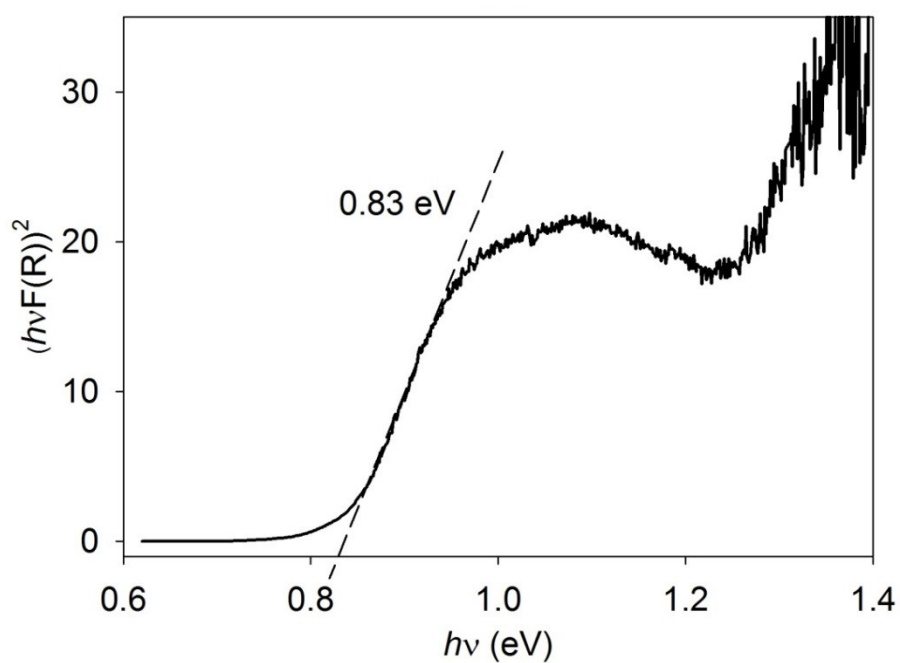
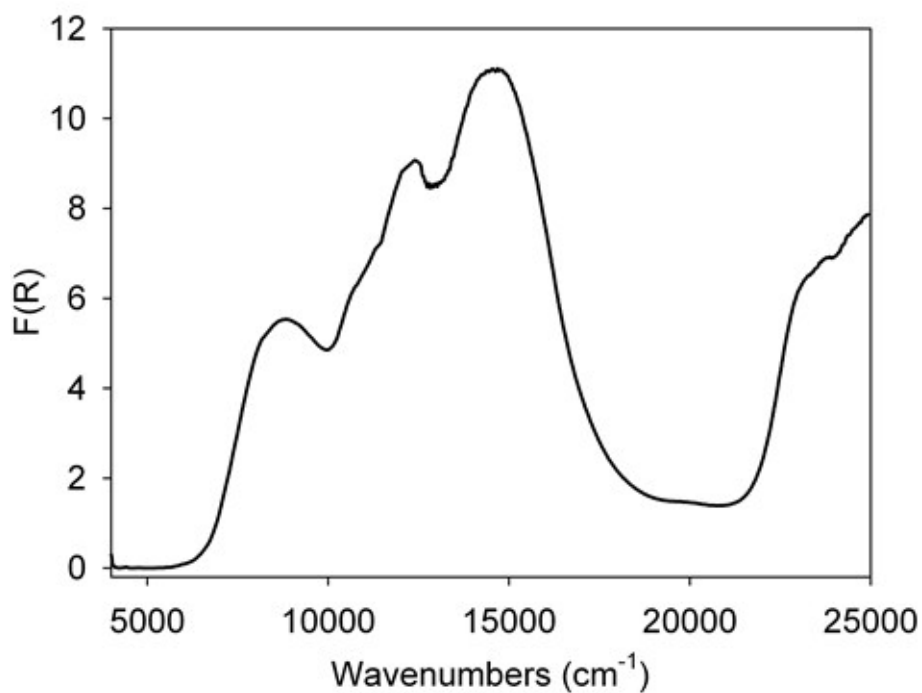


Fig. S6.11 a) The Vis-NIR solid-state diffuse reflectance spectrum of [(10)TCNQ]. b) The Tauc plot derived from the spectrum showing the estimation of the optical band gap.

a)



b)

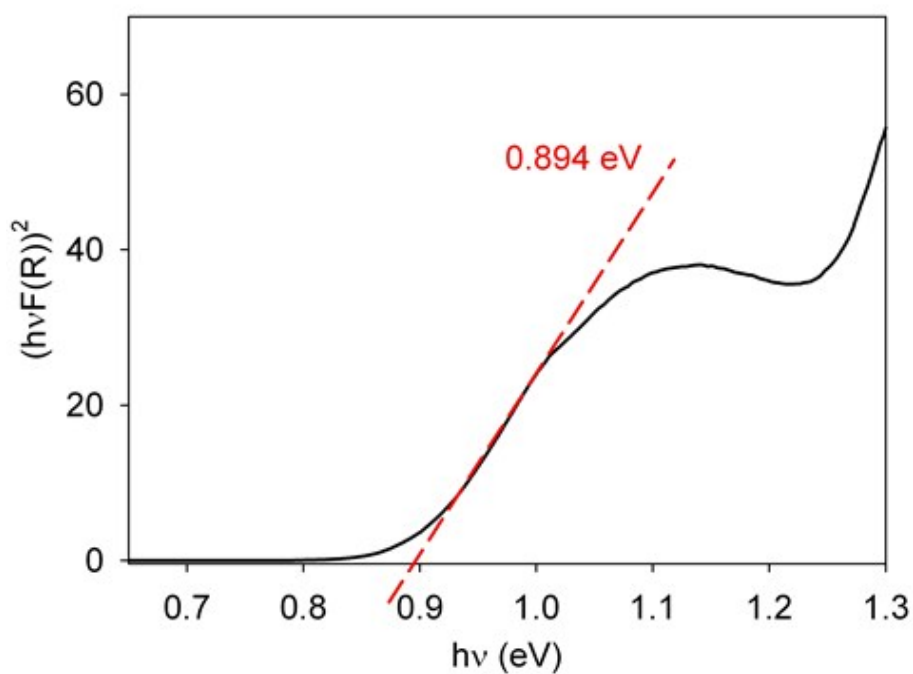


Fig. S6.12 a) The Vis-NIR solid-state diffuse reflectance spectrum of [(**10**)F₄TCNQ]. b) The Tauc plot derived from the spectrum showing the estimation of the optical band gap.